The Effect Of Wave Breaking On The Performance Of Tuned Liquid Dampers

The Effect Of Wave Breaking On The Performance Of Tuned Liquid Dampers

By Mohamed Omar, B.Sc.

A Thesis

Submitted to the School of Graduate Studies

In Partial Fulfillment of the Requirements For the

Degree of Master Of Applied Science

McMaster University

February 2015

Master Of Applied Science (2015) McMaster University

(Mechanical Engineering) Hamilton, Ontario

Tittle: The effect of Wave Breaking On The Performance Of Tuned Liquid Dampers

Author: Mohamed Omar, B.Sc. (University of Benghazi, Benghazi, Libya)

Supervisor: Dr. Mohamed S. Hamed

Number of Pages: IX, 56.

Abstract

An in-house numerical model developed at McMaster University was used in this research to investigate the effect of the wave breaking on the performance of Tuned Liquid Damper (TLD). In this model, the Volume Of Fluid VOF method was used to construct the free surface and the surface tension was taken into consideration to evaluate the wave breaking. The model was implemented on incompressible, 2D flow water within the TLD that was harmonically excited. . The ability of the TLD to cancel out the external excitation was examined via damping effectiveness of the TLD. The damping effectiveness is calculated as the ratio of the net energy experienced by the TLD to the input excitation energy; both energies were calculated as the area under the force-displacement curve. The investigation of the effect of the wave breaking was done through changing the fluid height ratios, amplitude and frequency ratios. The fluid height ratio was changed as h/L= 0.5, 0.35, 0.125 which is above and at and below the critical fluid level for wave breaking occurrence respectively. The critical height is defined as the height at which the waves start to break. It was found that at high fluid ratios wave breaking did not occur, in contrary, at critical level wave breaking did occur and even more breaking waves recorded to have taken place at much lesser levels. The effect of the fluid height ratio on the damping effectiveness of the TLD was investigated, it was seen that the damping effectiveness of the TLD improves as water level becomes shallower. The amplitude ratio was also examined; the behavior of the TLD in general did not change i.e. increasing the amplitude enhances the damping of the TLD. The frequency ratio range was selected to cover the near-resonance region. It was found that the TLD damps most excitation close to the resonance. The wave breaking occurrence was assured via the free surface visualization for several cases and found in agreement with different wave breaking shapes reported experimentally.

Acknowledgment

I am conveying my gratitude to Dr. Hamed for his amazing supervision and his patience and understanding and cheering me up at times I felt so depressed.

I also would like to acknowledge Dr. Tarek Oda that without his help my task would have been much more difficult.

I would like to thank my family, friends and critics who had a great support towards the completion of my thesis work.

Table of Content

List of Table

List of figure

Nomenclature

F(t)	Excitation force	(N)
H	Tank full height	(m)
h	Fluid height	(m)
L	Tank length in direction of excitation	(m)
γ	Mass ratio = $\frac{\text{Mass Of The Water}}{\text{Mass Of The Structure}}$	
Ω	Tuning ratio = $\frac{f_1}{f_s}$	
f_1	Natural frequency of the TLD	(Hz)
f_S	Excitation Frequency	(Hz)
u	Flow velocity in the x-direction	(m/s)
v	Flow direction in the y-direction	(m/s)
p	Pressure	(Pa)
τ	Shear stress	(Pa)
F	Volume of fluid	
ϕ	Potential function	
σ	Surface tension	(N/m)
μ	Dynamic viscosity	
WBP	Wave breaking probability	
FH	Fluid height	(mm)
f/f_1	Frequency ratio	
A/L	Amplitude ratio	
h/L	Fluid height ratio	

CHAPTER ONE

INTRODUCTION AND LITERATURE REVIEW

In the recent decades, the civil structures tend to be more taller and thinner, which make them much more susceptible to vibration caused by environmental external forces due to earthquakes and wind loadings. These external excitations could cause high levels of building acceleration, which could lead to structure damage and/or sense of discomfort for the building occupants. Numerous studies have been carried out to investigate ways to minimize the vibration caused by these forces. Dynamic Vibration Absorbers (DVAs) Frahm (1911) were introduced to mitigate vibration. One type of DVAs is known as the Tuned Liquid Damper (TLD), which is a tank filled with a liquid, most often being water. The excitation caused by external forces causes the water to slosh and as a result, "hopefully", anti-phasing the external excitation. Sloshing forces created by the movement of the water can either be in-phase with or anti-phase. The waves would break as they collide together or with the tank walls. The wave breaking effect is studied in the light of the TLD damping effectiveness by changing the parameters such as fluid heights h/L, Amplitude ratio A/L, Frequency ratio f/f_1.

1.1 The beginning of interest and implementation of TLDs.

TLDs have been widely used in fields of marine industry, spacecraft, and the idea was afterwards implemented to the earthbound structures. The mid of the nineteen century witnessed the first use of TLDs. The TLD was initially used as anti-rolling tanks that help in stabilizing the marine vessels against rough seas Honkanen (1990). In the 1960s, the same concept was used in Nutation Dampers used to stabilize a satellite in space [Bhuta (1966), Schneider (1973), Alfriend (1974)]. The offshore structures are vulnerable to wind, wave and

ocean currents, controlling the vibration of those platforms can be achieved by configuring the tankage of the required storage of water, fuel, mud and cruel oil Mitome (1979). Bauer (1984) was the first to implement the TLD in the structural engineering. Works related to use TLD in structure engineering were continued by Modi et al (1988), Fuji et al (1990), Kareem (1990), Sun et al (1992), Wakahara et al (1992).

1.2. Classification of Dynamic Vibration Absorbers (DVA)

To meet the serviceability criteria of tall structures, factors such as velocity, acceleration due to gust wind has to be considered. As mentioned previously, the dynamic vibration absorber (damper) is considered as one of the techniques used to accomplish this task. Dampers are basically an additional mass that is added to the primary structure and tuned to its frequency in order to mitigate its unwanted vibration and as such called Tuned Dampers. The dampers are primarily defined according to the power needed to activate them. The absorber that needs power to work is known as an active absorber. In this category, they are made of a relatively complicated system that encompasses receiving excitation details and analyzing them and then producing the proper reaction. The absorber whose functionality does not require external source of power is referred to as a Passive Absorber (e.g. Tuned Mass Dampers (TMD), Tuned Liquid Dampers (TLD)). The last category is called semi-active dampers. As the name suggests, it is neither an active nor passive damper, however, the energy requirement order of magnitude is less than the typical active dampers.

Before proceeding in details on the passive dampers, it is worth mentioning some other techniques used to overcome such structural vibrational problems. The protection systems of structural vibration are summarized in Table (1.1) Soong (1997).

Table 1.1 Types of Vibration Protection Systems

Passive Energy Dissipation	**Semi-active and active control**	**Seismic Isolation**
Metallic Dampers	Active Bracing Systems	Elastomeric Bearings
Friction Dampers	Active Mass Dampers	Lead Rubber Bearings
Viscoelastic Dampers	Variable Stiffness or Damping Systems	Sliding Friction Pendulum
Viscous Fluid Dampers		
Tuned Mass Dampers	Smart Materials	
Tuned Liquid Dampers		

The advantage of having an active absorber is due to their smart design and the way they react in case of applied excitations as they can change the system damping characteristics depending on the nature of excitation and as such providing greater performance levels. As those systems potentially require power supply, any shortage in this source make them useless devices, and their relative high cost makes them less attractive compared to the passive dampers. The focus of this study is on TLDs, which are passive dampers. Due to the analogous concept of the Tuned Liquid dampers (TLD) with the Tuned Mass Dampers (TMD), it is helpful to go over the underlying facts of those dampers.

1.2.1. Tuned Mass Dampers

One of the fundamental yet powerful mechanisms in controlling the structural vibration is the Tuned Mass Dampers “TMD”. The TMD is simply an additional mass attached to the main

structure to create an anti-phase force. Consider the system in figure (1.1) where the structure is of a mass m_1 subjected to an external excitation F(t).

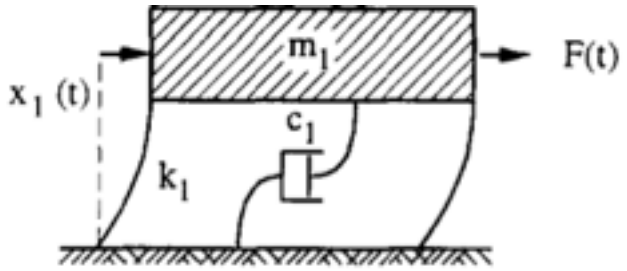

Figure (1.1) Simple structure system Kwok, B. S. (1995).

The amplitude of the system response with and without a TMD is shown in Figure (1.2). There, the system amplitude increases gradually and proportional to the frequency ratio (excitation frequency to natural frequency) until the excitation frequency equates the natural frequency of the structure (resonance). At resonance the amplitude becomes infinity; afterwards, the amplitude starts to decay once the excitation exceeds the system natural frequency. Adding a TMD makes the amplitude of the structure goes to almost zero at resonance, which is the main objective of using the TMD. Nevertheless, instead of having one resonance point, there will be two resonance points, which are expected since the system is now a two Degree of Freedom (2DOF) system.

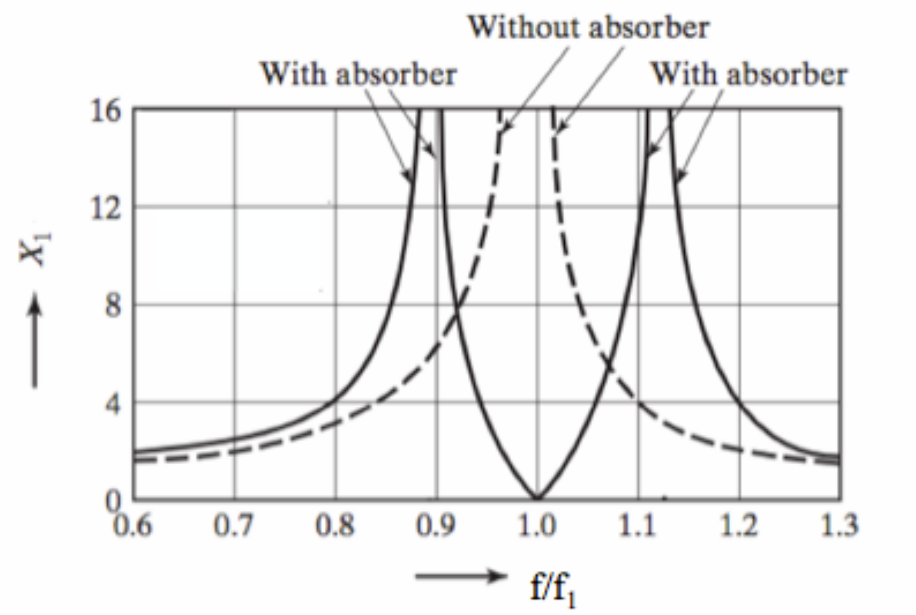

Figure (1.2) the structure system response with and without absorber Rao (2011)

In order to make the damper more practical device, that is TMD works for a broad band of excitations, the TMD should be damped (i.e. adding a dashpot for damping purposes) C_2 in Figure (1.3). In this configuration the TMD reduces the structural amplitude considerably and it is no longer depends on the resonance point (solid line in Figure (1.4)).

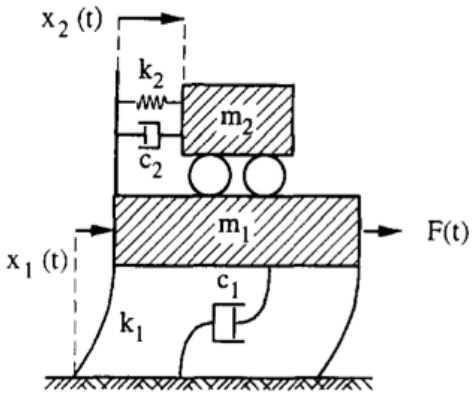

Figure (1.3) Structure-TMD system Kwok (1995)

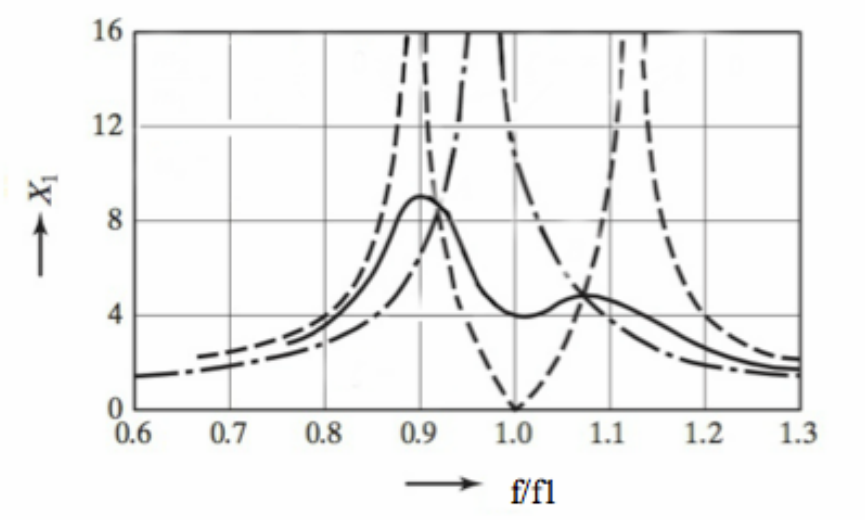

Figure (1.4) Response of structure- damped with TMD Rao (2011)

An example of TMD is the one implemented in Taipei 101 as shown in Figure (1.5). It weights 660 metric tons and of a diameter of 5.5 m, and it is located between the 91th and 87th floors. This TMD is expected to reduce the building sway caused by gust wind by up to 40% Taipei-101 (2009).

Figure (1.5) Taipei 101 TMD Taipei-101 (2009)

1.2.2. Tuned Liquid Dampers

Tuned Liquid Dampers are passive dampers. A TLD is a tank filled with liquid usually water at certain level, h, as depicted in Figure (1.6). In the figure, H is the tank full height, L is the tank length in the direction of excitation, h is the liquid initial height. The departure from the free surface as result of the motion of the fluid is denoted as η.

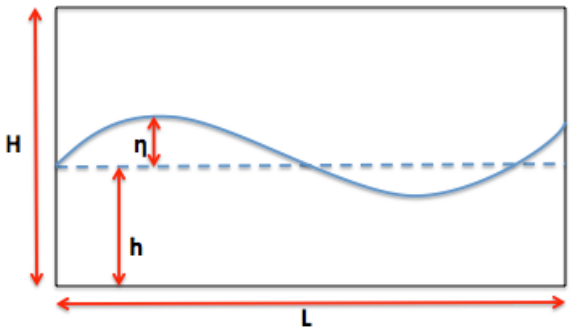

Figure (1.6) Schematic of the TLD

Once the building starts experiencing external excitations such as wind excitation, the water sloshes in such a way that would counteract the applied load as long as the natural frequencies of both the structure and the attached TLD are synchronized Lamb (1945). TLDs are categorized based on the container used as Tuned Sloshing Dampers and Tuned Liquid Column Dampers (TLCD). TLDs are classified according to the initial liquid height into two classes. When the fluid height ratio h/L is less than 15% the TLD is classified as shallow TLD, however, when h/L exceeds this ratio, the TLD is classified as a deep TLD Kareem (1993). The deep TLD has low damping characteristics in comparison to the shallow TLD. The main source of damping in the deep TLD is the fluid viscosity, which was proven to be ineffective Sun (1991). The shallow TLD offers more damping due to the wave breaking, however, due to the large number of TLDs that need to be installed to meet the required mass ratio and the limited space available for them, the deep TLD are used after implementing techniques like adding screens that enhance the damping of the deep TLDs. TLDs are designed in different geometries; the geometry of the TLD is practically determined by the space availability. The geometry of the TLDs could be any

ordinary shape, e.g. rectangular TLD [Chang (1999), Sun et al (1992)], square TLD Bhattacharjee et al (2013), or conical TLD Casciati (2003), cylindrical TLD Tamura et al (1995), or could be of irregular configuration as in case of limited spaces Tait et al, (2012). A Tuned Liquid Column Damper (TLCD) is shown in Figure (1.7). The TLCD combines the effect of liquid motion in a tube, which results in a restoring force using the gravity effect of the liquid, and the damping effect caused by loss of hydraulic pressure created by orifice. TLCD can be U-type TLCD Hitchcock et al (1997) or V-type TLCD Gao et al, (1997). An example of TLCD is the one implemented in One Wall Center in Vancouver. Due to the absence of the orifice in the typical TLD and because the mere effect of wave breaking is sought, the focus is on the TLD. Although the concept of the TLD seems straightforward, the nature of the fluid movement makes this type of absorbers somehow tough to be comprehended because of the non-linear behavior of the flow. On the other hand, the low capital cost, the less need for maintenance and space requirements compared to TMDs as well as the ability to tune for a variety of frequencies make this type of absorbers more favorable over the TMDs. Example of TLD is One King West Building In Toronto Canada.

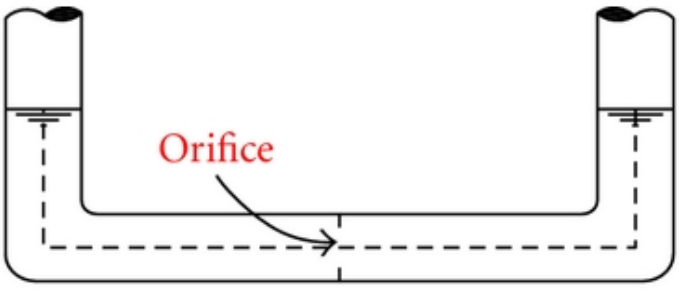

Figure 1.7 TLCD

The TLD is experiencing different types of excitations; the two main types of excitation that dealt with in literature are wind loading, Earthquake loading. The effect of wind loading is an

important factor that should be taken into account prior starting constructing civil structures. A tremendous work has been dedicated towards studying the impact of adding TLDs to civil structures experiencing wind loading [Tait et al (2010), Wang et al (2011), Zhang et al (2009)]. The earthquake is another "threat" to building's stability. Although the earthquake lasts for short time compared to wind loading, its effect needs to be taken into consideration [Jin et al (2007), Banerji (1999), Banerji (2011)].

1.2.3. Analysis of the TLDs

In order to fully understand the concept of the TLD, there are few parameters that have to be highlighted and comprehend. To the author's best knowledge, the TLD has been investigated via two approaches, namely, Experimental Approach, Numerical approach.

1.2.3.1 TLD performance parameters

The Tuned Liquid Damper performance can be defined via the following parameters:

Mass ratio

The ratio of the mass of the TLD to the structure mass is known as the mass ratio (γ).

$$\gamma = \frac{\phi^2 * m_{TLD}}{M^*} \quad 1.1$$

Where ϕ^2 is the normalized model deflection of the structure at the position of the TLD, and m_{TLD} is the TLD mass, which can be obtained using the linear potential theory as follows:

$$m = \frac{8 \tanh\left(\frac{\pi h}{L}\right)}{\frac{\pi^3 h}{L}} \quad 1.2$$

Where h is the liquid initial height, L is the tank length in the direction of the excitation, and M^* is structure generalized mass

Tuning ratio

By tuning the TLD to the structure's frequency, the fluid absorbs the vibrational energy created by the external excitation via sloshing. The tuning ratio is defined as:

$$\Omega = \frac{f_1}{f} \tag{1.4}$$

Where f_1 is the damper natural frequency, which can be obtained for rectangular tanks using the following equation (Lamb, 1932).

$$f_1 = \frac{1}{2\pi}\sqrt{\left(\frac{\pi g}{L} * tanh\left(\frac{\pi h}{L}\right)\right)} \tag{1.5}$$

f : The excitation frequency $(\frac{1}{s})$

1.2.3.2.Experimental Approach

The analogy of the TMDs and TLDs was investigated to simplify the analysis of TLDs. Those kinds of models are commonly represented by the mass-spring-damper system undergoing an external excitation. The liquid within the tank is broken into multi-masses where each mass symbolizes the different sloshing modes Figure (1.8)

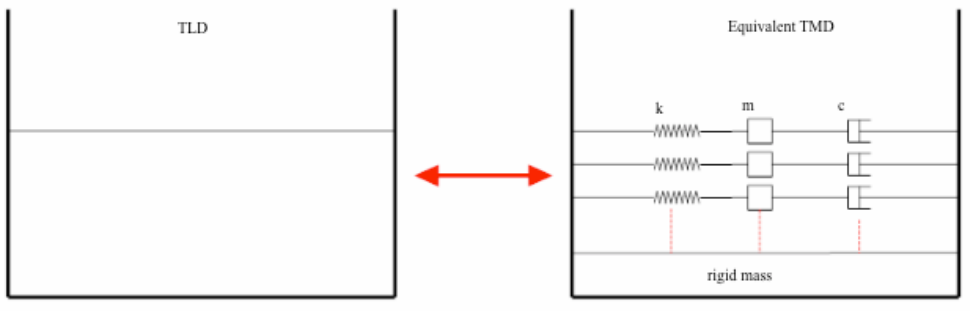

Figure 1.8 TLD-TMD Analogy

[Graham (1951), Graham (1952)] they were the pioneer researchers who engaged in the treatment of the sloshing taking place inside the tanks using the mechanical models. Kareem (1987) implemented that equivalent mechanical model to simulate the TLD that was outfitted with a high building that was subjected to earthquake excitation. Chang (1999) have experimentally studied the effectiveness of the TLD in mitigating the vibration on tall buildings caused by vortex-excited forces. A series of wind tunnel experiments on different TLD geometries were examined. They proposed a TLD frequency ranges between 0.9 and 1 of that of the building model and a mass ratio of 2.3%. It was concluded that rectangular TLD is the perfect geometry in damping the excitation. With the aid of the TLD-shaking table interface force, the nonlinear model of the TLD was established via equivalent mass, damping ratio and frequency ratio Sun et al (1995). Later on, Yu experimentally modeled the TLD as a TMD by considering the mass as constant and named it as Nonlinear Spring-Damper (NSD). The equivalent damping and stiffness were obtained by matching the energy dissipated by the TLD and that of the NSD Yu (1997). The approach was used to simulate the conical TLD. The equivalent TLD parameters (frequency, mass, damping) were depending on the fluid level within the TLD, and graphs were plotted showing the dependency of the frequency and damping on the amplitude and fluid heights Casciati (2003).

1.2.3.3. Numerical Approach

The problem associated with fluid flow analysis inside tanks is the nonlinearity caused by the free surface of those fluids, and therefore a special treatment for those parts of the fluid field has to be considered. The numerical flow analysis in tanks is performed by dividing the fluid within the tank into tiny cells (meshes); other technique that is “meshless”. The first attempt of evaluating the free surface flow problems was the Marker-And-Cell method (MAC) [McKee, et

al (2007), Welch (1965)]. The method is based on Eulerian frame where the fluid volume is represented by a set of marker particles. The cell that includes a marker is deemed to carry a fluid and visa versa. The free surface using this method is defined as that the cell includes at least a marker and it is neighbor does not is a free surface cell. The problem of this method, though, is in the amount of computer memory storage required to store the coordinates of each particle moving with the fluid per cycle. This problem is solved by another technique called Volume of Fluid (VOF). Assigning a factor F whose value varies from 0 to 1 that represents the volume fraction of the fluid in the flow mesh cells. The value of F=1 means that the cell is occupied entirely by fluid, while F=0 stands for empty cells, the values in between is where the free surface cells are located. Using the factor F reduces the storage memory requirement of the code since all the fluid cells volume will have the same factor defining their values Hirt (1981). Another approach for tracking free surface is used named Level Set Method (LSM). It uses a function whose value is equal to zero at the free surface and by differentiating with respect to time an update for the free surface is achieved Price (2006). The three previous methods are Mesh-based or Eulerian prescription is used to define the flow domain. Lagrangian formulation is used in the Smoothed Particle Hydrodynamics (SPH) method. The method relies on the idea of dividing the flow region into particles instead of meshes thus no boundary conditions are required at the free surface and consequently can capture phenomena such as wave breaking Monaghan (1988). This method was widely used to investigate the sloshing in tanks undergoing rolling motion; the problem with this method is that it is computationally expensive [Souto Iglesias, et al (2004), Souto-Iglesias, et al (2006), Delorme, et al (2009), Fang, et al (2009)].
A detailed description of the two fundamental equations (the momentum equation as well as the continuity equation) is deferred to the next chapter. There have been assumptions on the use of the abovementioned equations in the analysis of the TLDs. The shallow water theory was used to

simulate the flow inside tanks. The wave height or the amplitude of the interfacial deformation is assumed to be small compared to the mean depth of the liquid layer, and the horizontal velocity is uniform throughout the depth, and as result this theory fails to simulate free surfaces Reed et al (1998). The linearized form of the Navier-Stokes equation was used to simulate the sloshing within a rectangular tank. This approach neglects the convective term. This term has however a profound effect in case of strong sloshing which made it less desirable technique to investigate the TLD at sever sloshing events Lepelletier (1988). Another study that deals with modeling the TLD equipped with submerged nets. The flow equation of motion was solved based on the assumption of potential flow field and no account was given neither for the fluid viscosity nor the wave breaking Kaneko (1999). M.R. Siddique and his colleagues suggested a model to simulate the nonlinear TLD. The model that relies on the vorticity-stream function, it takes into its account the viscosity and was meant for the 2D sloshing in a rectangular tank. A comparison was made between the model and an experimental data, and an excellent agreement was noticed. The fluid was assumed to be viscous, and incompressible Siddique et al, (2004). In 2009, a numerical model was developed by Marivani to investigate the 2D, viscous, incompressible flow without any linearization, the model developed by Marivani did not consider the surface tension on the free surface and as such it is not capable to predict the wave breaking Marivani (2009).

1.3. Review of literature.

Once the liquids inside containers are excited, they will no longer be still; therefore, their free surface becomes interrupted and waves created as result of momentum change and that what is known as sloshing phenomena. The water sloshing has received an extensive attention during the past few decades due to its profound influence on systems' stability. For instance, the liquid sloshing within cargos, Liquefied Natural Gas (LNG) containers, and oil transportation vehicles can "jeopardize" the safety of the structures and accordingly their crews. However, this dissertation focuses on exploiting the sloshing phenomenon to work in favor of stabilizing the vibrating structures. The knowledge of the natural frequencies helps in good design of sloshing tanks, which is the manifestation of applied techniques in evaluating the free surface of those containers. Wave is defined as the movement of the water with a certain periodic back-and-forth and/or up-and-down motion. The fluids in shallow, open containers experiencing external excitations will have different waves in their free surface. The waves created as a result of roll motion as shown in Figure 1.9. The fluid initially exhibits a stationary status then wave is called standing wave [form (1)]. Increasing the frequency a group of small waves starts to travel from right to left of the tank [form (2)]. A hydraulic jump takes place as soon the frequency increases further [form (3)]. Increasing frequency causes the bore to travel [form (4)] and eventually transforms to solitary wave [form (5)] Bones (1968). Although that those forms of waves are due to rolling motion, but can similarly happened in the sway motion as per the factors governing the different patterns are mostly frequency, amplitude and fluid height Bouscasse (2013). Water waves are transmitted either at water body (body waves) or at surface (surface waves). While the first propagates within the fluid the second travels in two mediums (e.g. water-air), and need a restoring force that causes wave propagation Lin (2008).

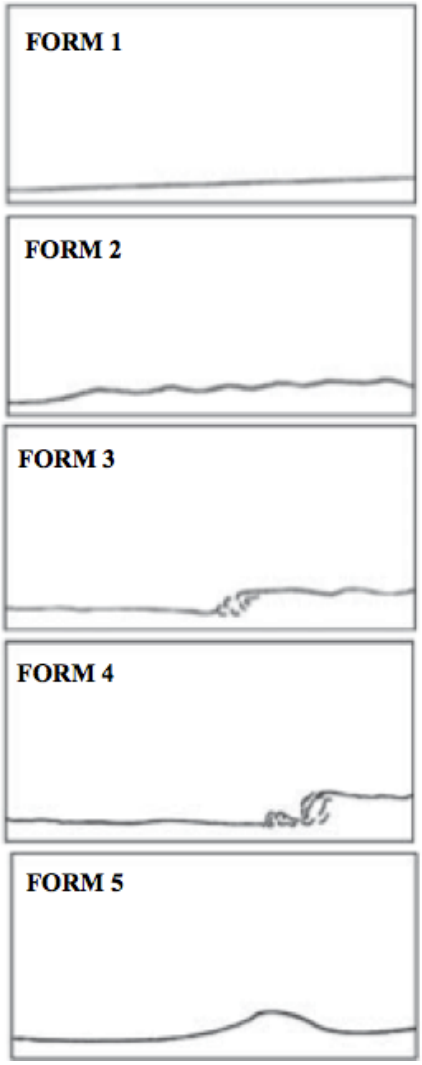

Figure 1.9 Wave forms Bones (1968)

A phenomenon happens at the free surface called wave breaking, which is the cornerstone of this research, is of great importance when analyzing the free surface waves. Wave breaking can be defined as a rapid transition associated with turbulence Reed, et al (1998). The shallow water theory was used to simulate a rectangular TLD experiencing sway motion assuming that free surface is a continuous surface (no wave breaking) Sun, et al (1989). Later on, the model was developed to take into its account the wave breaking via empirical coefficient. According to the author, the damping increased due to wave breaking which is represented by the coefficient C_{da}.

Experiments have been conducted in order to determine the value of the coefficient and found that C_{da} is function in the motion amplitude Sun (1994). Lagrangian-based method known as Moving Particle Semi-Implicit (MPS) was used to simulate wave breaking. This method is based on fluid particle interactions. It was however, used to investigate wave breaking on sloped surfaces such as shores for non-viscous fluids SeiIchi et al (1997). The MPS method suffers from pressure fluctuation due to mistakenly considering particles having low to zero pressures as free surface particles. Therefore, a method was developed and called Consistent Particle Method (CPM). The method shows an excellent compatibility with the experimental work in term of visualizing wave breaking Mimi (2011). SPH method was used to evaluate the sloshing within rectangular tank undergoing sway and rolling motion. The SPH method, which is based on representing the fluid domain by a number of particles each have a mass and move according to the force applied on the whole system, showed a good agreement with the experiment that sought sloshing force to inertial force ratio as a function of the forced oscillation period, and free surface wave time history. The wave breaking was captured at Amplitude of 0.028 m, and fluid height h= 0.173 m. both numerically and experimentally Colagrossi et al ~~Lugni~~ (2004). Colagrossi collaboratively with others conducted a study on sloshing in rectangular tank. The study was done numerically using SPH method, and experimentally using rectangular tank of dimensions of 1m for height and length and of 0.1m width (dimension against line of motion). The fluid height within the tank was 0.35m (slightly higher the critical depth for wave breaking to takes place). They investigated changing the excitation periods close to the natural periods and a group of amplitudes ranging from 0.03 to 0.1m. For the suggested periods and amplitudes assigned, four different scenarios were recognized namely (see Figure (1.10)):

1. No wave breaking
2. Alternative wave breaking

3. Long time randomic asymmetric breaking
4. Local splashing jets

The first category resembles the normal flow without breaking. Increasing either period or amplitude leads free surface to fragment. The second group appears to have more than one configuration as the name already indicates. Breaking mostly occurs in the sides of the tank for all excitation periods considered. More severe breaking happens near the middle of the tank as the amplitude increases, and that is the third group. The last category is when the jet formed and splashed little away from the wall.

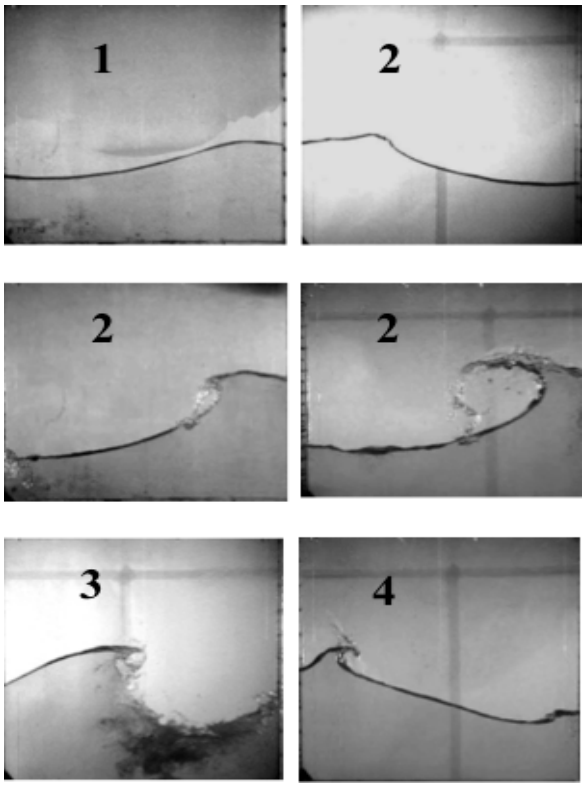

Figure 1.10 Wave breaking category Colagrossi et al (2004)

1.4.The objective of the present work

In this work the main focus is about the effect of the wave breaking created within the TLD due to the wind excitation on the performance of the TLD, the current work is concerned with two points:

1. Visualizing wave breaking instances at different parameters and comparing them to experimental wave breaking grades presented in Figure (1.10).
2. Studying the effect of the wave breaking under various fluid height ratios, frequency ratios and amplitude ratios via the damping effectiveness

Chapter Two

Mathematical Formulation

2.1. Introduction

The TLD that is being considered in this research is a rectangular tank of a width L in the direction of the excitation, and a height H. It carries water to a certain level h. The depth d of the tank is considered to be 10 times less than the width to ensure two-dimensionality Figure (2.1). The tank is subjected to a harmonic external excitation with amplitude A, and frequency f.

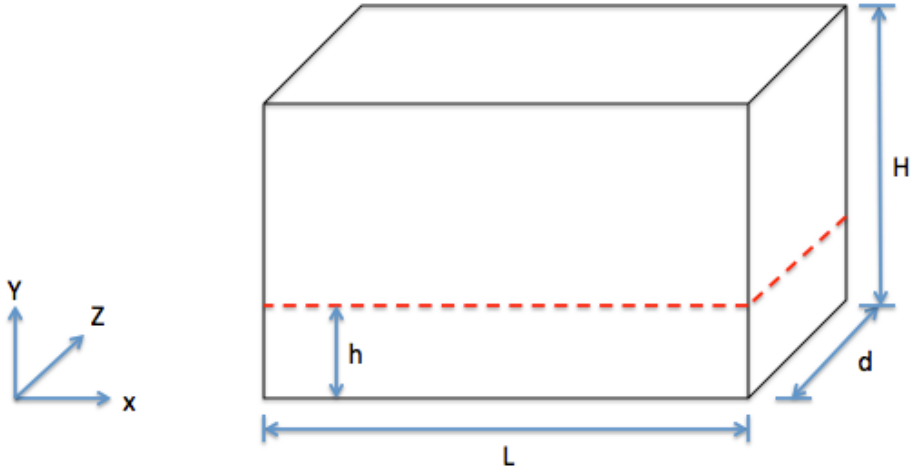

Figure 2.1 TLD Dimensions

The dimensions of the tank considered in this investigation are as follow:

Table 2.1 Dimensions of the TLD

Tank Dimensions (m)	
Fluid height (h)	0.5, 0.35, 0.125
Width (L)	1
Depth (d)	0.1

The TLD dimensions selected here are based on the dimensions used in the experiments carried out by Colagrossi (2004).

2.2. Governing Equations

The water is treated as a Newtonian, incompressible fluid with a free surface. The two-dimensional motion of the water is governed by the following conservation of mass and momentum:

Conservation of mass equation

$$\frac{\partial u}{\partial x}+\frac{\partial v}{\partial y}=0 \qquad 2.1$$

Conservation of momentum equation

$$\frac{\partial u}{\partial t}+u\frac{\partial u}{\partial x}+v\frac{\partial u}{\partial y}=g_x-\frac{1}{\rho}\frac{\partial P}{\partial x}+\frac{1}{\rho}\frac{\partial \tau_{xx}}{\partial x}+\frac{1}{\rho}\frac{\partial \tau_{xy}}{\partial x} \qquad 2.2$$

$$\frac{\partial v}{\partial t}+u\frac{\partial v}{\partial x}+v\frac{\partial v}{\partial y}=g_y-\frac{1}{\rho}\frac{\partial P}{\partial y}+\frac{1}{\rho}\frac{\partial \tau_{yy}}{\partial y}+\frac{1}{\rho}\frac{\partial \tau_{xy}}{\partial y} \qquad 2.3$$

The airside is taken into consideration via the free surface boundary conditions. The time evolution of the free surface due to the external excitation is resolved using the following Volume of Fluid (VOF) equation Hirt (1981).

$$\frac{\partial F}{\partial t}+u\frac{\partial Fu}{\partial x}+v\frac{\partial Fv}{\partial y}=0 \qquad 2.4$$

Here F is a function that represents the fluid volume fraction within the cell. For cells of F values between 0 and 1, the cells are considered as a free surface cells as long as they have at least one empty neighbored cell. On the other hand, the cell is named as a water cell when F equals unity, while it is a void or air cell when F is equal to zero. To advect F function, the

Donor-and-Acceptor method is used. At the boundary of the successive cells, the cell that delivers flow is denoted as a Donor Cell and carries a subscript D whereas the cell that receives flow is denoted as an Acceptor Cell and have a subscript A, and accordingly each cell will have four different subscripts depending on the flow direction that is determined based on the sign of the velocity vector. Horizontally, for example, the cell (i,j) is a donor cell when the velocity at its right-hand face is greater than zero Figure (2.2).

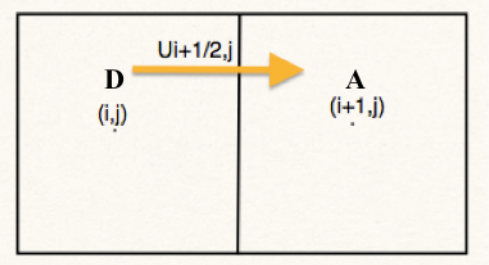

Figure 2.2 Donor-and-Acceptor Cells

The most updated velocity is used to determine the advected amount of F across the cell face. The gradient of the F estimates the free surface orientation. Once the free surface slope and the F value of the waterside are known, a line is constructed representing an approximation of the actual free surface.

2.3. The Boundary Conditions

The TLD flow domain has three solid boundaries (bottom, left and right sides) and a free surface. The boundary conditions for the flow are the velocity and pressure boundary conditions. At the solid surfaces, the no-slip and no-penetration conditions are applied. The pressure boundary conditions are evaluated on the sides of the tank. The pressure condition at the bottom of the tank is the hydrostatic pressure, which is estimated via the fluid height (h) as

$$P_{bottom} = \rho g h \qquad 2.5$$

The pressure condition at the sides, however, is estimated using the equation

$$P_{side} = \alpha * e^{-(\frac{y}{h})} * \sin(\omega * t) \quad 2.6$$

Where α is the pressure maximum amplitude determined by nature of the external excitation. The last equation has been developed based on the experimental work done to evaluate the pressure distribution on the wall in the direction of excitation that indicated that the pressure on them change in the same manner as the external excitation Panigrahy et al (2009). At the free surface, the stress boundary conditions are applied in the normal and tangential directions. The stress boundary condition in the normal direction

$$p - \sigma k = 2\mu n_k \frac{\partial u_k}{\partial n} \quad 2.7$$

The stress boundary condition in the tangential direction

$$\mu\left(t_i \frac{\partial u_i}{\partial n} + n_k \frac{\partial u_k}{\partial s}\right) = \frac{\partial \sigma}{\partial s} \quad 2.8$$

Where:

$\frac{\partial}{\partial n} = \hat{n}.\nabla$ is the normal derivative.

$\frac{\partial}{\partial s} = \hat{t}.\nabla$ is the surface derivative.

Where σ is the fluid surface tension. Considering the free surface as a very thin layer that is the viscous effects are insignificant, subsequently, the right hand side of equation 2.7 vanishes. This indicates that the dominant factor is the surface tension in the vicinity of the free surface. As far as the free surface is concerned as per the occurrence of wave breaking, the Continuum Surface Force (CSF) model is used in the current numerical work to represent the surface tension Brackbill (1992). This model assumes that the interface as a very thin layer within which the fluid is characterized via a function $c(\vec{x})$ as follows:

$c(\vec{x}) = c_1$ for liquid,

$c(\vec{x}) = c_2$ for air,

$c(\vec{x}) = \langle c \rangle = (c_1+c_2)$ for the interface 2.9

The fluid characteristics could be any fluid feature such as density. The model handles these properties using smoothed variation function $\tilde{c}(\vec{x})$ of the fluid properties from the waterside to the airside over a distance O(h*), h* is a transition layer thickness that is related to the mesh size. The deformation happening on the free surface as a result of the sloshing, however, can not be accurately simulated using the smoothed function, alternatively, the CSF model uses the volume force and by using the delta function as following:

$$\lim_{h\to 0} \int_{\Delta v} \vec{F}_{sv}(\vec{x})\, d^3 x = \int_{\Delta v} \vec{F}_{sa}\,(\vec{x}_s)\, d s \qquad 2.10$$

The last equation is based on the Green Theorem that states that the integration of the volume force around the volume of the interfacial region is equal to the integration of the surface force around the interfacial area Δs. The former force, surface force $\vec{F}_{sa}$, consists of the normal and the tangential components described as:

$$\vec{F}_{sa} = F_S^n\, \hat{n} + F_S^t\, \hat{t} \qquad 2.11$$

As mentioned earlier, the tangential forces are negligible and accordingly the only force effect is due to the surface tension, which leads to

$$\vec{F}_{sa} = F_S^n = \sigma\, k(xs)\, \hat{n}(xs) \qquad 2.12$$

Finally, the surface force (due to surface tension) is added to the body force F_b in the momentum equation.

2.4. Prediction of wave breaking

At the free surface there are two conditions that have to be met in order to formulate the wave breaking. The first is the velocity boundary condition, and the second is the stress balance condition. The velocity boundary of the free surface was given based on the assumption of the equality of vertical component of velocity across the interface between water surface and the adjacent air that is represented as following

$$v_{Liquid} = v_{air} = \frac{\partial \eta}{\partial t} + u\frac{\partial \eta}{\partial x} + v\frac{\partial \eta}{\partial y} = 0 \qquad 2.13$$

For ideal fluids and ignoring the viscosity effects, the hydrodynamic pressure of the excited fluid is described via the following equation Bhattacharyya (2010)

$$\frac{p(x,y,t)}{\rho_f} = -\left\{\frac{\partial \phi}{\partial t} + \frac{1}{2}|\nabla\phi|^2 + g\eta\right\} \qquad 2.14$$

Equation (2.14) is based on the potential flow theory, where the atmospheric pressure is zero on the free surface, ϕ is the potential function and η is the elevation over the fluid still level h. The current model replaces Bernoulli's equation by another formula, which gives accountant of the viscous stresses and body forces. The fluid displacement in the vertical direction (i.e. η) is calculated as follows Ibrahim (2005):

$$\eta = \frac{1}{g}\frac{\partial \phi}{\partial t}\Big]_{y=h} \qquad 2.15$$

Differentiating equation 2.15 with respect to y leads to

$$\frac{\partial \eta}{\partial y}\Big]_{y=h} = \frac{-h}{\rho g}\frac{\partial^2 p}{\partial y^2}\Big]_{y=h} \qquad 2.16$$

In order to take the viscous forces effect into consideration, equation (2.16) uses the Possion equation to evaluate the pressure gradient, which carries the viscous term, which will be illustrated in the next chapter. The wave breaking forms shown in Figure (1.10) have a common

feature that is the folding of the crest on itself. The free surface can be visualize via stream function as φ (x,y,t), and accordingly at the free surface the streamline will fold on itself as a result of the wave breaking that point is known as "Reflection Point". Mathematically speaking, at the location of the reflection point, the second order deferential of the stream function will vanish, and consequently

$$\left[\frac{\partial^2 \mathrm{p}}{\partial \mathrm{y}^2}\right]_{\text{at the reflection point}} = 0 \qquad 2.17$$

Equation 2.17 is the criterion used in this model to postulate the wave breaking taking place within the TLD.

Chapter Three

The Numerical Model

The current model is in-house numerical model, which was developed to study the wave breaking phenomenon within TLDs. This model is developed for 2D, incompressible flows with free surface within rectangular tank as shown in Figure (3.1). The tank is represented in Eulerian domain of M cells. The flow field governing equations are discretized using the finite difference technique. The finite difference convention follows the MAC scheme, where the scalar quantities are evaluated in the center of the cell such as pressure and volume of fluid F, whereas the vector quantities are evaluated on the boundaries of the cells Figure (3.1).

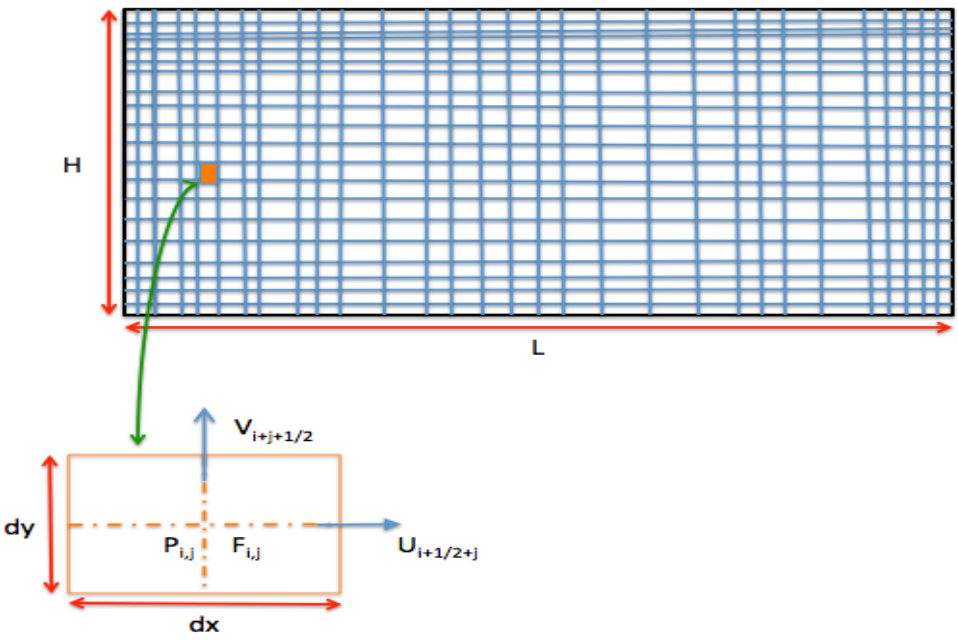

Figure 3.1 The mesh representation

In Figure (3.1), the (i,j) stand for the center of the cell, and as such the velocities in the horizontal direction U, and vertical direction V are located at the right (i+1/2,j) and top

(I,j+1/2) faces, respectively. The dimensions of the cell are represented on the element as dx and dy.

3.1. The Numerical Model

The momentum equation is solved using the Two-Step Projection Method. This method was introduced in the middle of the twentieth century, and is based on the Helmholtz Decomposition Chorin (1968). The time discretization of the momentum equation is

$$\frac{\vec{V}^{n+1}+\vec{V}^{n}}{\partial t}+\nabla.\left(\vec{V}\vec{V}\right)=-\frac{\nabla P^{n+1}}{\rho}+\frac{\nabla.\tau^{n}}{\rho}+\vec{g}+\frac{\vec{F}_{b}^{n}}{\rho} \quad 3.1$$

The main idea is to split the momentum equation into two parts as follows:

$$\frac{\tilde{V}-\vec{V}^{n}}{\partial t}=-\nabla.\left(\vec{V}\vec{V}\right)+\frac{\nabla.\tau^{n}}{\rho}+\vec{g}+\frac{\vec{F}_{b}^{n}}{\rho} \quad 3.2$$

$$\frac{\vec{V}^{n+1}-\tilde{V}}{\partial t}=-\frac{\nabla P^{n+1}}{\rho} \quad 3.3$$

The projection method first solves the convection-diffusion equation to predict the intermediate velocities, equation (3.2), which is then projected onto the space of divergence-free field, equation (3.3). The link between the momentum and the continuity is through the Poisson's equation as following

$$\frac{\nabla.\tilde{V}}{\partial t}=\nabla.\left(\frac{\nabla P^{n+1}}{\rho}\right) \quad 3.4$$

The former equation (equation 3.4) was extracted by combining equation 3.3 with the continuity equation.

3.2. Flow Chart of the Algorithm

The procedure of solving the flow field within the TLD consists mainly of the following steps:

1. Finish the preliminary steps such as (generating mesh, inputting numerical and fluid

parameters, initializing the free surface)

2. Solve the continuity and momentum equation using the provided boundary conditions

3. Update the F function to determine the fluid configuration at the new time step.

4. Examine the wave-breaking criterion on the free surface.

5. Calculate the sloshing force.

6. Increment the time step, and start new cycle.

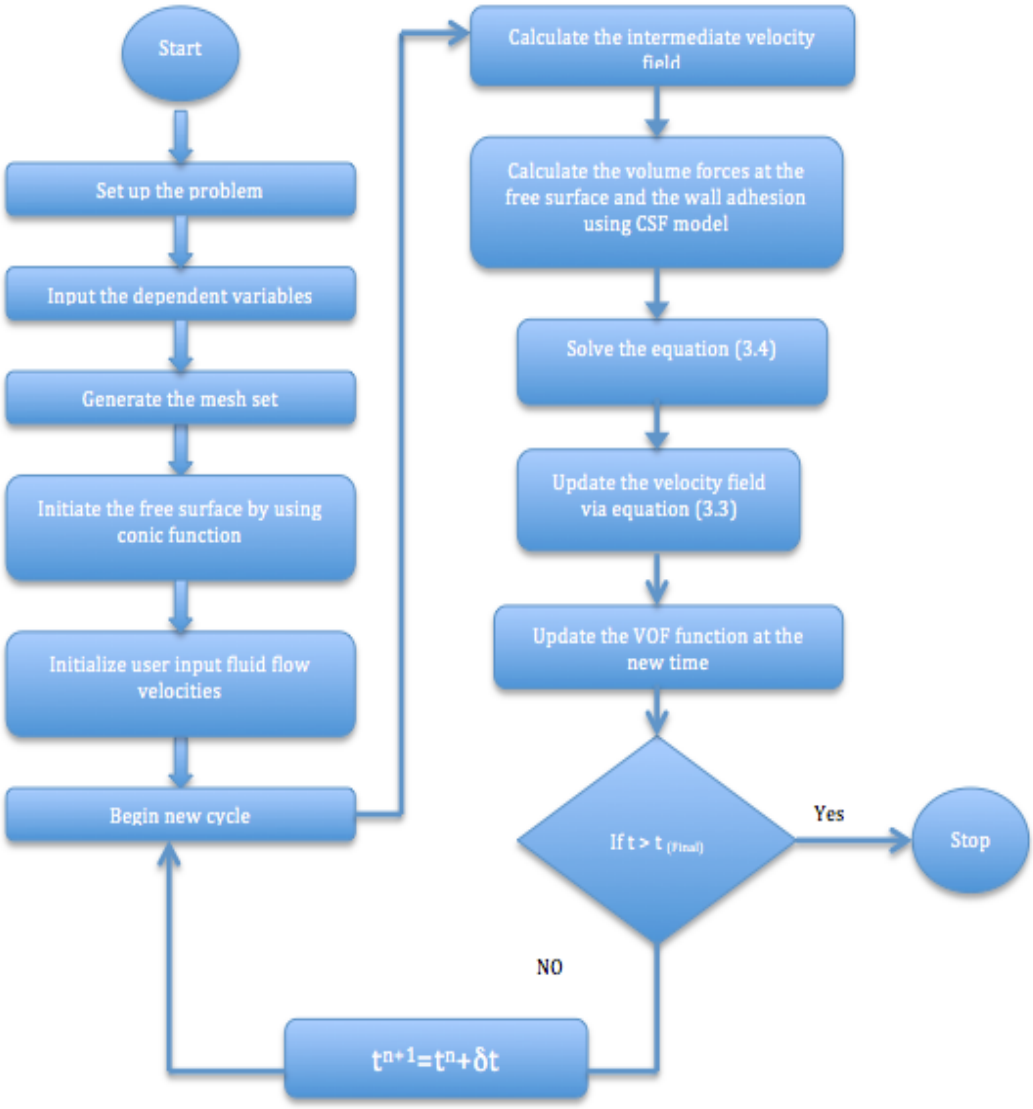

Figure 3.2 Algorithm flowchart

3.3.Validation of the Numerical Model

3.3.1. Free Surface

The code used in this research has been validated using experimental data reported in Colagrossi et al (2004) and Colagrossi et al (2010). Colagrossi performed water sloshing experiments on a tank with the dimensions of 1m length, 1m height and 0.1m width. The tank was exposed to excitation in the x-direction. The displacement of the external excitation can be described by the relation $x=A*\sin(\omega*t)$ where A is the excitation amplitude and ω is the angular velocity, and t is time. Two cases were used to validate the current model. One case was at a fluid height ratio h/L=0.35, and an amplitude ratio of A/L= 0.05, and the other was at h/L=0.125 and A/L=0.03, both cases have the same frequency ratio of 1.15.

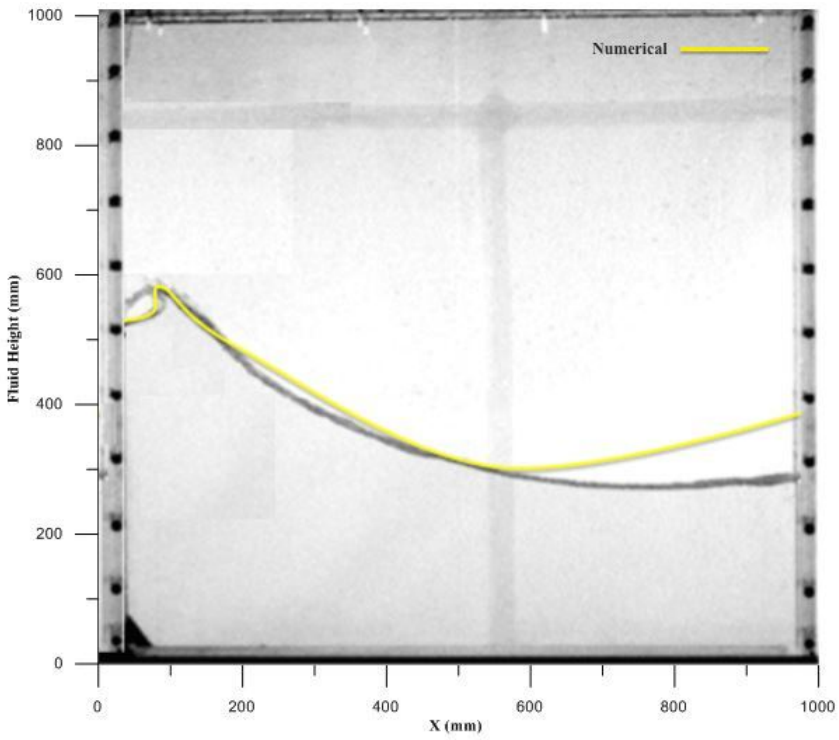

Figure 3.3 Comparison between experimental results reported in Lugni et al (2004) and the current numerical results for the case of h/L=0.35, A/L=0.05, f/f1=1.15 at t=1.23 sec.

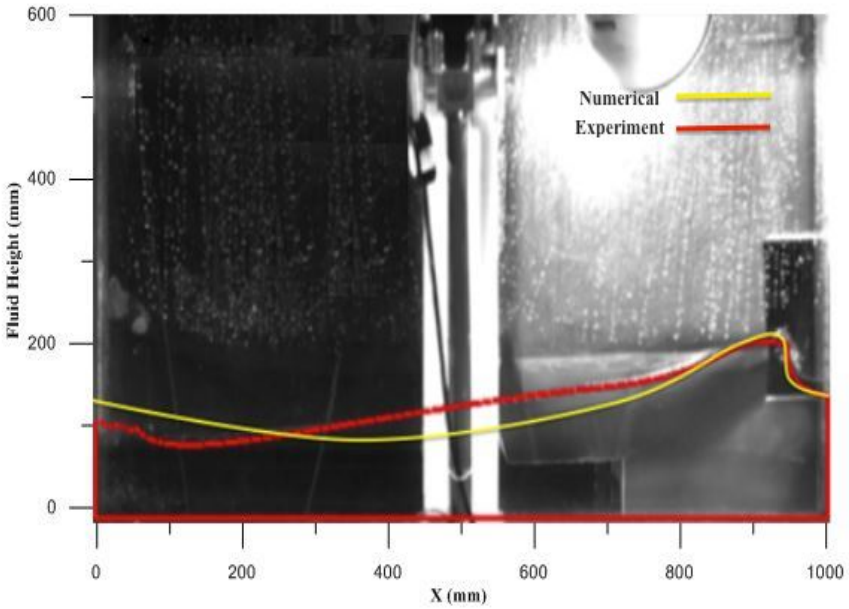

Figure 3.4 Comparison between experimental results reported in Colagrossi et al (2010) and the current numerical results for the case of h/L=0.125, A/L=0.03, f/f1=1.15 at t=4.43 sec.

Figures 3.3 and 3.4 show a comparison between the numerical and experimental results. The maximum deviation of the numerical free surface from the experimental one is about 20%. Although there is discrepancy in the free surface at locations away from breaking; nevertheless, results shown in Figures 3.3 and 3.4 confirm the ability of the current model to represent the occurrence of the wave breaking as seen at the location of its onset which is a very important aspect for the current study.

3.3.2. Pressure Time History

The pressure variation on the left wall of the TLD was examined experimentally for a tank of dimensions of 200 mm (width), 400 mm (Length) and 800 mm (Height) and a water level is 140 mm via a pressure sensor. The ability of the current numerical model in evaluating the pressure on the same wall of the tank at 24 mm from the bottom was examined.

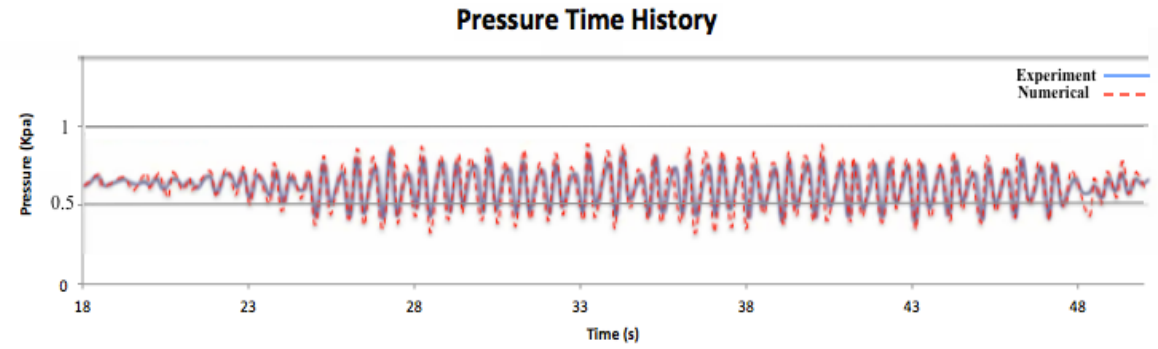

Figure 3.5 TLD left wall pressure time history (Experiment vs Numerical) at f= 7 Hz and A/L= 0.0675 mm Mohamed et al (2014).

From Figure 3.5 the numerical model evaluation of the pressure time history is almost similar to the experimental evaluation with small deviation along the time span.

CHAPTER FOUR

RESULTS AND DISCUSSION

4.1. Introduction

In this chapter, the effect of the frequency ratio (f/f1), amplitude ratio (A/L) and fluid height (h/L) on the occurrence of wave breaking and the damping performance of the TLD is investigated using the current model. The effect of wave breaking on the damping performance of the TLD is investigated using the following damping effectiveness:

$$\text{Damping effectiveness} = \frac{\text{Net energy}}{\text{Excitation energy}} \quad 4.1$$

The energy is calculated from the area under the force-displacement curve. The net energy is the difference between the energy due to the external excitation force and the sloshing force. The displacement is described by the harmonic motion as $x=A^* \sin(\omega^* t)$, where A is the excitation amplitude (m). The TLD reduces the excitation that is represented in the positive values of the damping effectiveness. However, the TLD helps the excitation as shown in the negative damping effectiveness. The wave breaking criterion discussed in chapter 2, was used to determine the occurrence of wave breaking. Since the zero can not be represented as the numeric value of 0, the effect of the numerical value of zero has been investigated using 10^{-6} and 10^{-8}. Figure 4.1 and 4.2 show the effect of the numerical zero on the probability of wave breaking. The wave breaking probability (WBP) is the total time of occurrence of wave breaking moments divided by the total simulation time. The wave breaking probability has been examined at all fluid levels mentioned in Table 2.1, nevertheless, wave breaking was most observed at fluid levels of 0.35 and 0.125, and as such will be used to represent the WBP in Figure 4.1 and 4.2.

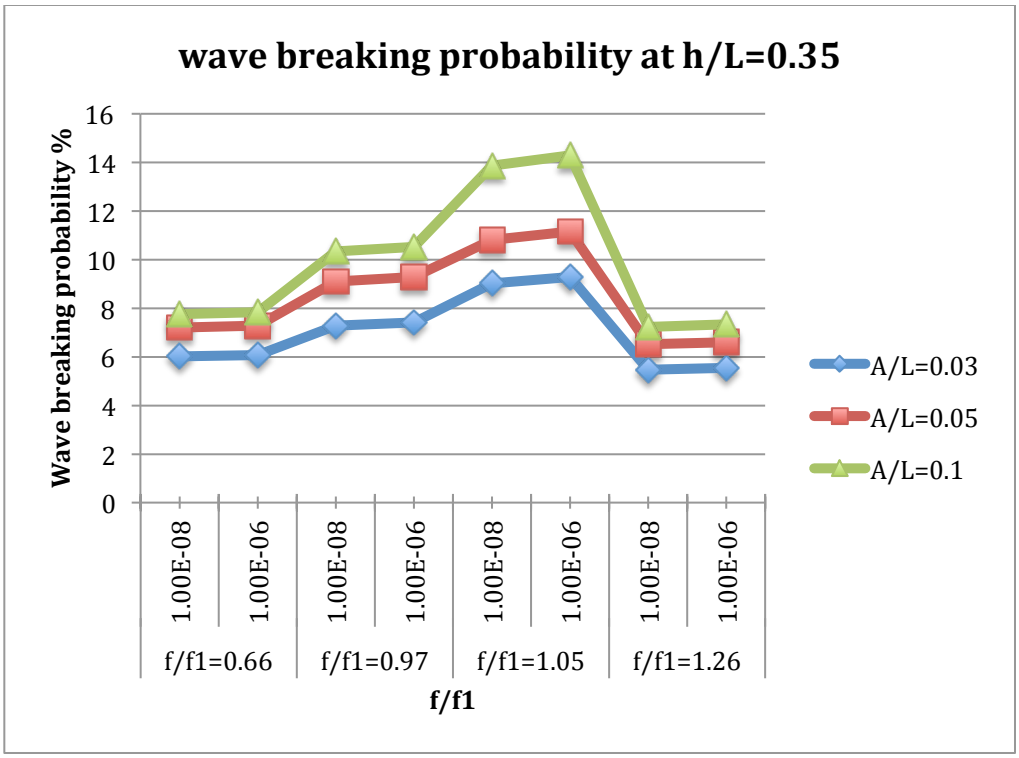

Figure 4.1 Wave breaking probability at h/L=0.35

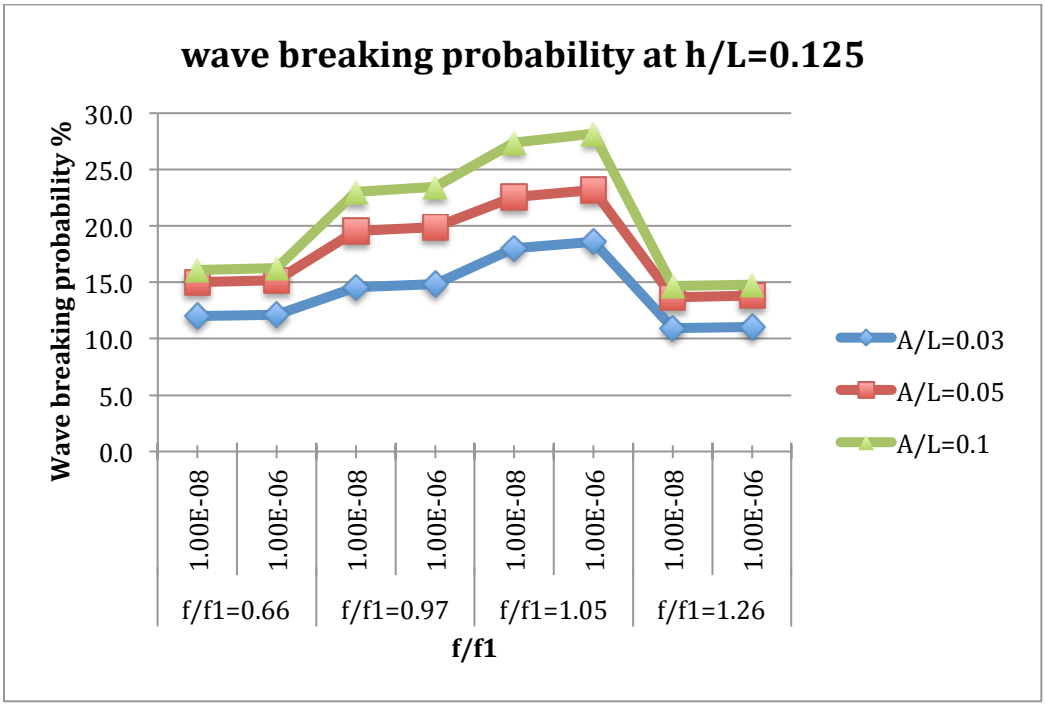

Figure 4.2. Wave breaking probability at h/L=0.125

From the figures above, it is clear that there is a small difference between the two numerical zeros where the maximum difference is 3%. The 10^{-8} was used in all cases reported here.

4.2. Mesh Independence Test

The effect of the mesh size on the numerical results was tested using three mesh sizes. Table 4.1 shows the difference in damping effectiveness obtained for the three mesh sizes for the case h/L=0.125, A/L=0.1 and f/f1=1.05. This case was selected because of the wave breaking occurred the most.

Table 4.1 Mesh Dependence Test

Mesh size	X nodes	Y nodes	Difference in damping effectiveness
Finer	200	100	1%
Coarser	66	30	10%
Reference	114	60	-

The reference mesh size was changed, the resultant difference in damping effectiveness percentage is relatively small for finer mesh, therefore, it is concluded that the current model mesh is independent.

4.3. Sample of Wave Breaking Instances Predicted by The Current Numerical Model

The wave breaking is the existence of the free surface discontinuity; in this section certain snapshots of wave breaking are presented. The significant of presenting those snapshots is to link between the grades of the wave breaking early shown in Figure (1.10), and the free surface topologies given by the current model. The free surface for the two fluid

level ratios, namely; 0.35 and 0.125 are represented. According to the wave breaking probability, the higher the amplitude, the more the wave breaking is, and as such A/L=0.1 was selected, and examined at different frequency ratios. The wave breaking occurrences at the different cases are listed in Table 4.2 and 4.3 for h/L=0.35 and 0.125 respectively.

Table 4.2 Wave breaking incidents at h/L=0.35, A/L=0.1

Wave breaking Incident	X (mm)	Y(mm)	T(sec)
f/f1=1.26	798	432	12.1
f/f1=1.05	112	478	9.72
f/f1=0.97	519	371	6.62
f/f1=0.66	591	456	13.42

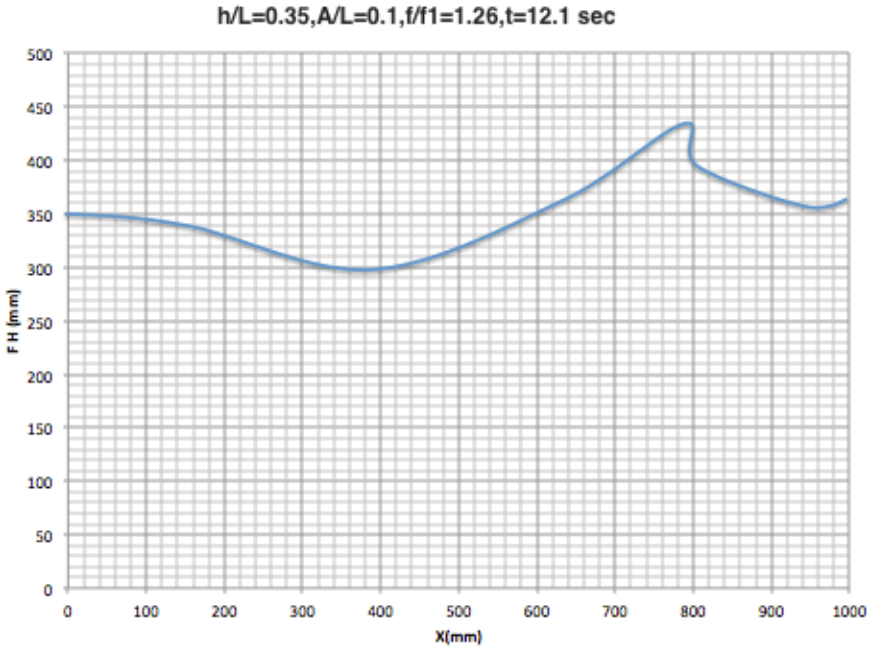

Figure 4.3. Free surface at h/L=0.35, A/L=0.1, f/f1=1.26, t=12.1 sec

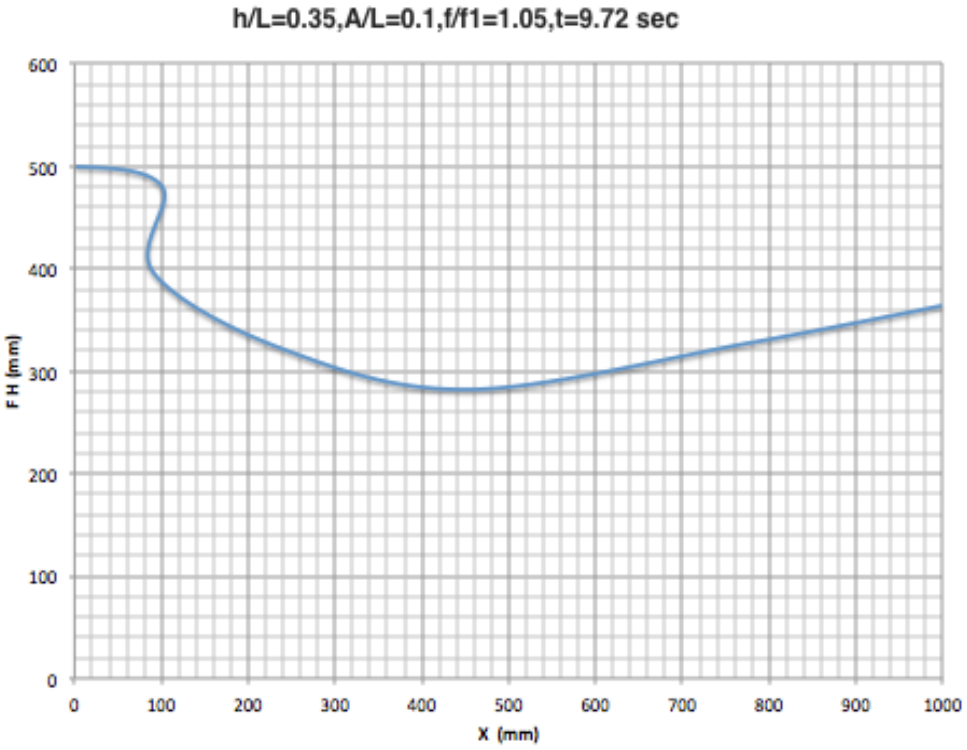

Figure 4.4. Free surface at h/L=0.35, A/L=0.1, f/f1=1.05, t=9.72 sec

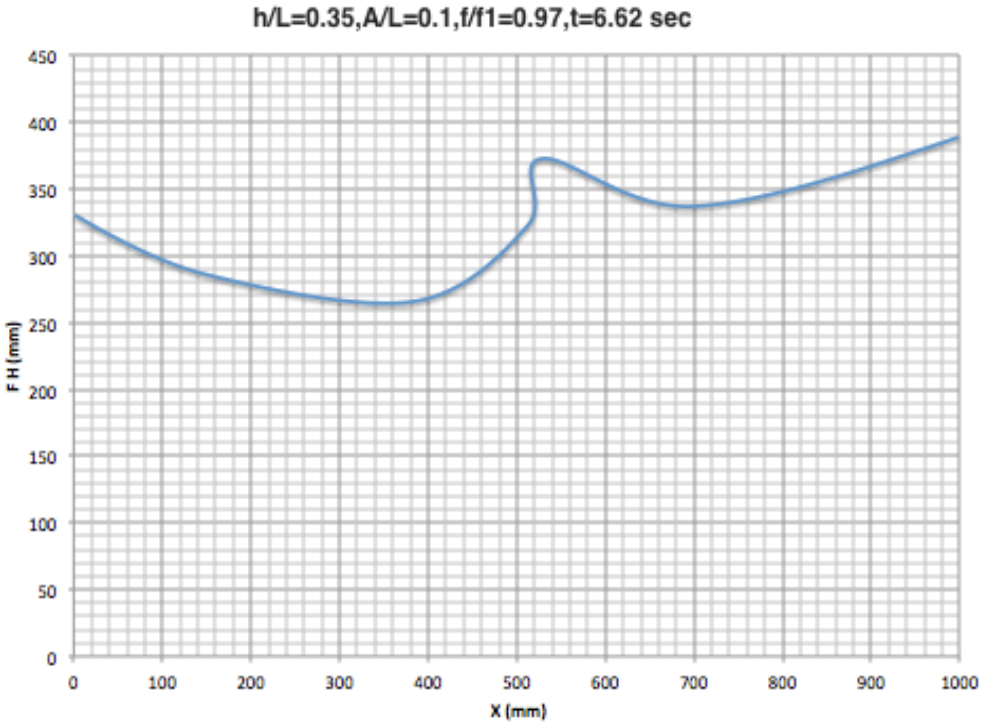

Figure 4.5. Free surface at h/L=0.35, A/L=0.1, f/f1=0.97, t=6.62 sec

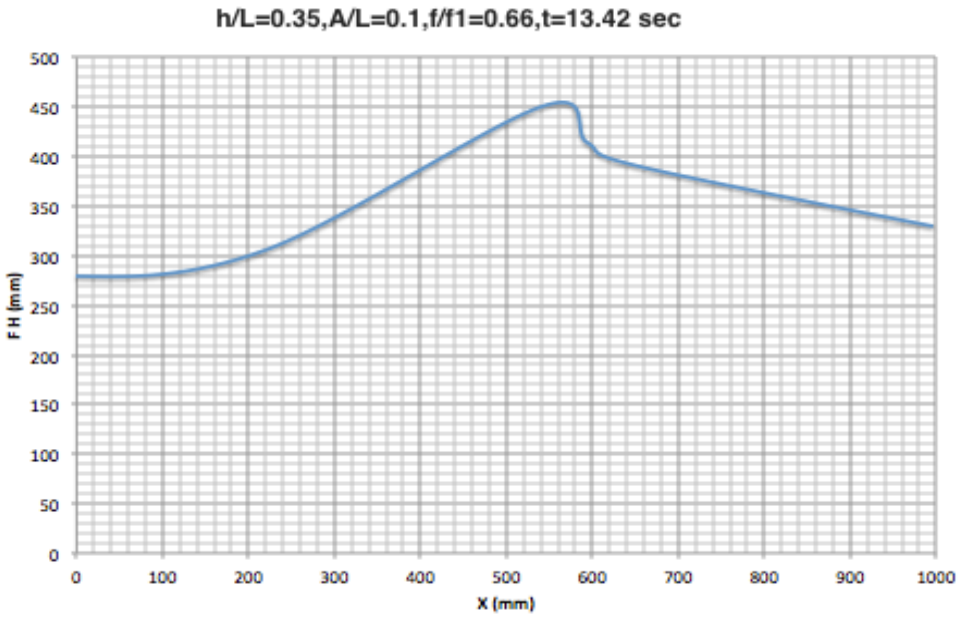

Figure 4.6. Free surface at h/L=0.35, A/L=0.1, f/f1=0.66, t=13.42 sec

The wave breaking occurred in Figure 4.3 through 4.6 having grades between 3 and 4, which are breaking at the middle of the tank and plunge near the wall respectively.

For the shallowest level, the free surface is drawn for the range of the frequency ratio used as it was done for previous fluid level h/L=0.35, the wave breaking details are listed in table 4.2

Table 4.3 Wave breaking incidents at h/L=0.125, A/L=0.1

Wave breaking Incident	X (mm)	Y(mm)	T(sec)
f/f1=1.26	558	143	6.01
f/f1=1.05	982	168	11.5
f/f1=0.97	442	147	11.3
f/f1=0.66	227	136	8.12

The wave breaking grades early presented in Figure (1.10) for this level were noticed,

however, in Figure (1.10) the run-up was not mentioned, which was noticed throughout the cases run in this study

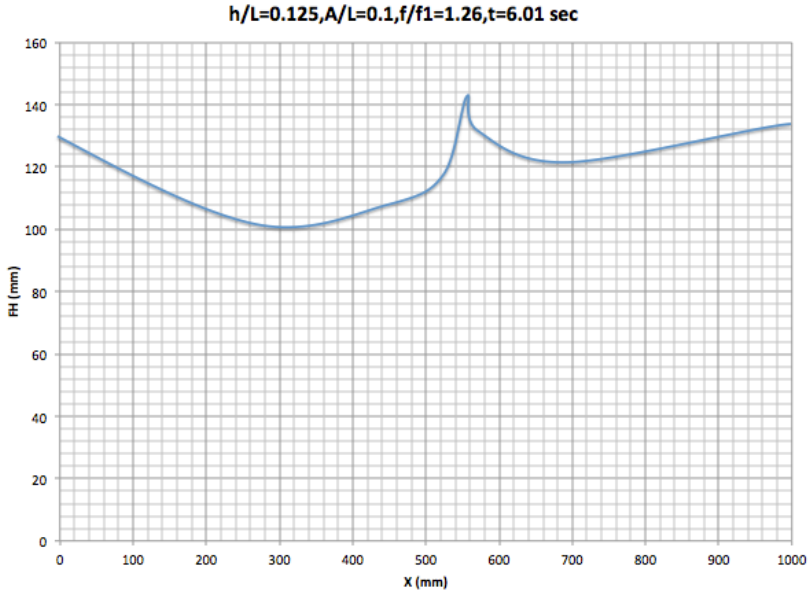

Figure 4.7 Free surface h/L=0.125, A/L=0.1, f/f1=1.26, t=6.01 sec

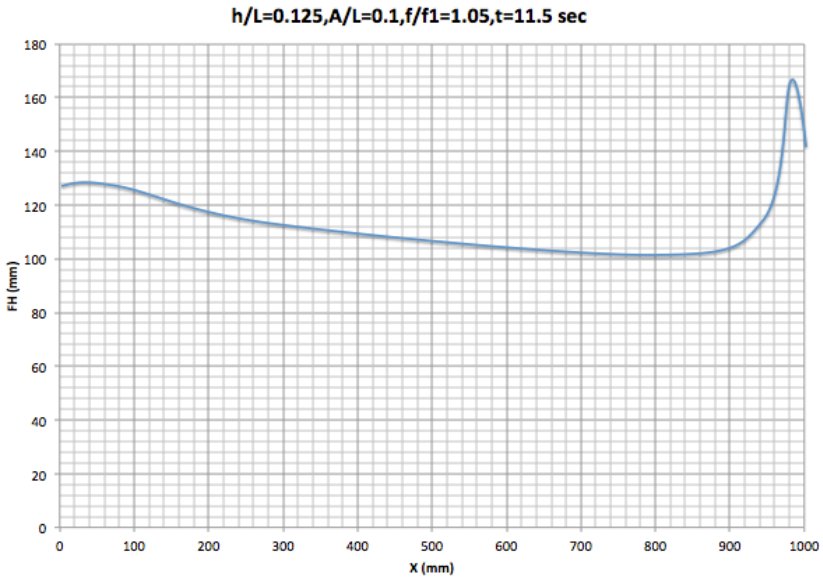

Figure 4.8 Free surface h/L=0.125, A/L=0.1, f/f1=1.05, t=11.5 sec

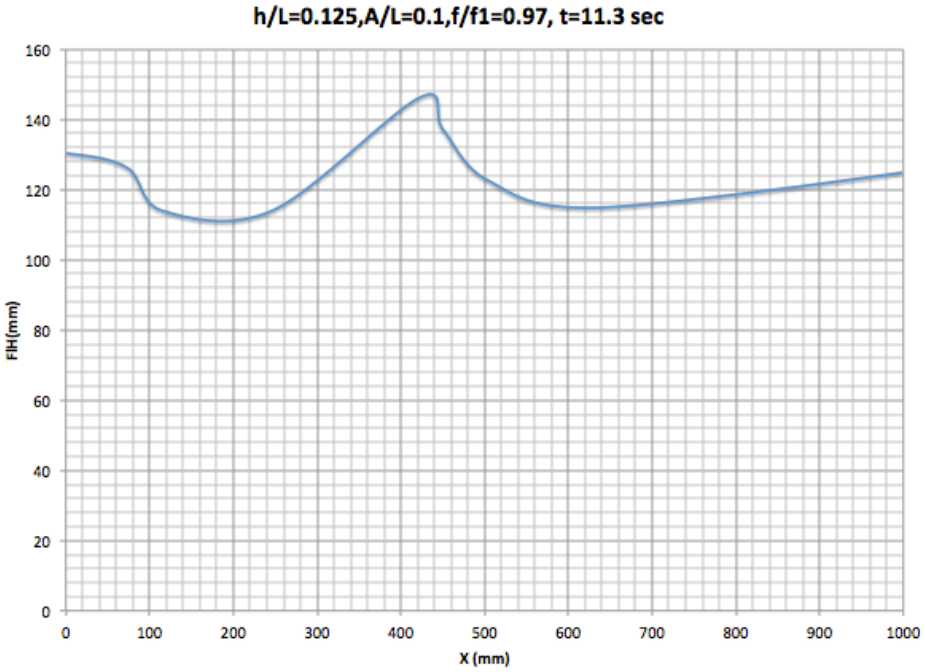

Figure 4.9 Free surface h/L=0.125, A/L=0.1, f/f1=0.97, t=11.3 sec

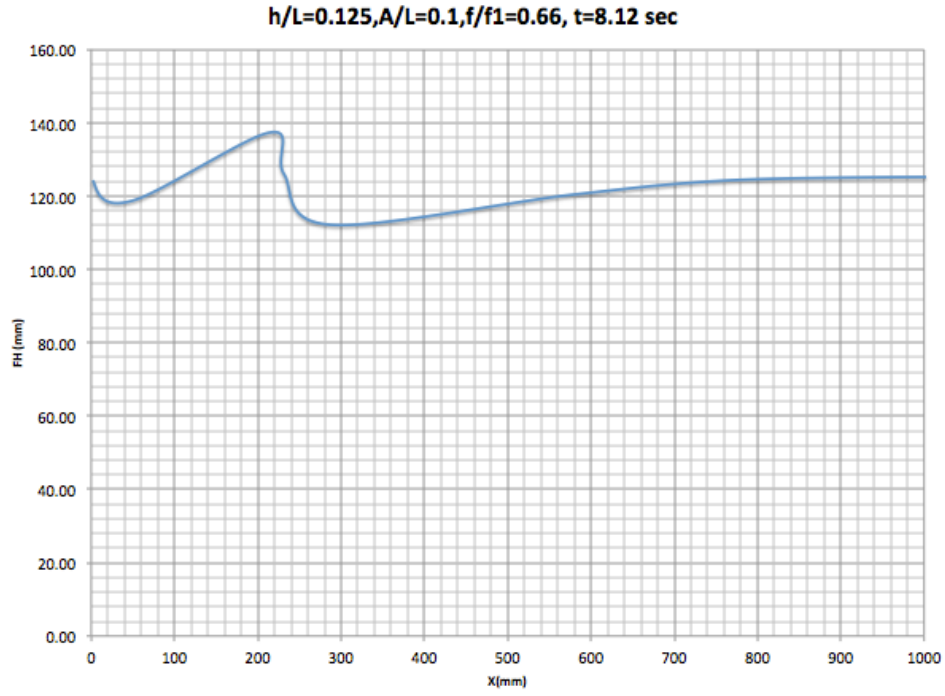

Figure 4.10 Free surface at h/L=0.125, A/L=0.1, f/f1=0.66, t=8.12 sec

It is worth mentioning that at all cases for the levels h/L=0.35 and 0.125, all different wave breaking grades in Figure (1.10) were noticed regardless of the frequency and amplitude ratios.

4.4. Effect of Fluid Height:

Because wave breaking was observed experimentally at low fluid heights, the effect of wave breaking on TLD damping was investigated at three different liquid levels; h/L= 0.5, 0.35 and 0.125. These fluid heights were selected based on the experimental work done by Colagrossi (2004). Figures (4.11-4.14) are depicting the effect of the fluid height on the TLD damping at different frequency and amplitude ratios.

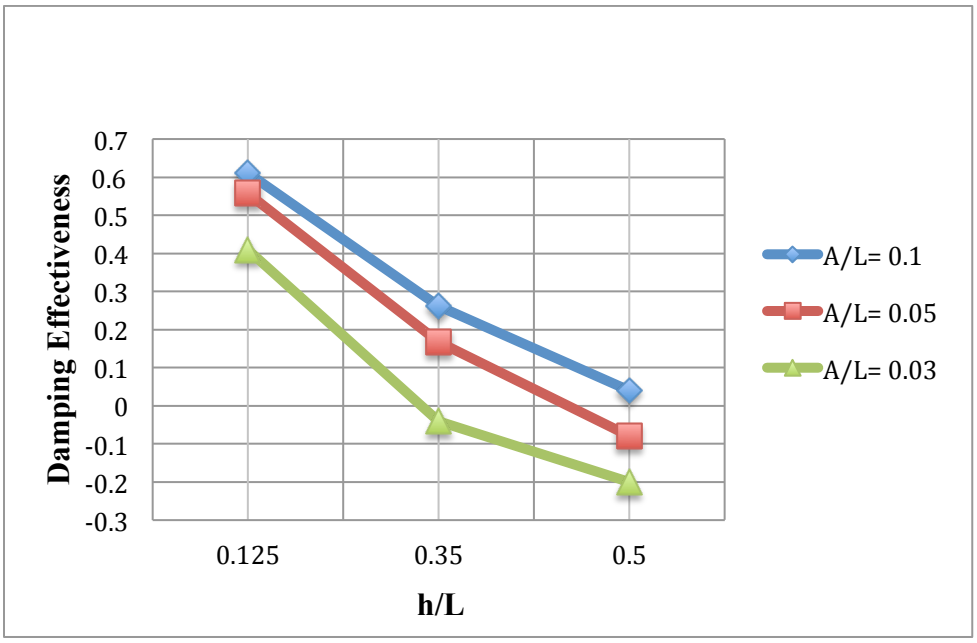

Figure 4.11 Effect of fluid height on TLD damping at f/f1= 0.66 and all A/L

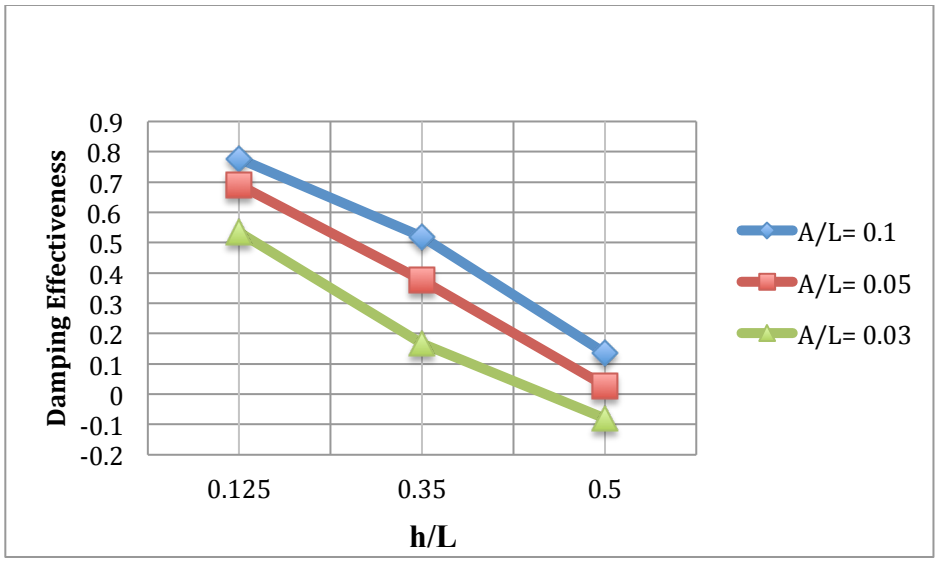

Figure 4.12 Effect of fluid height on TLD damping at f/f1=0.97 and all A/L

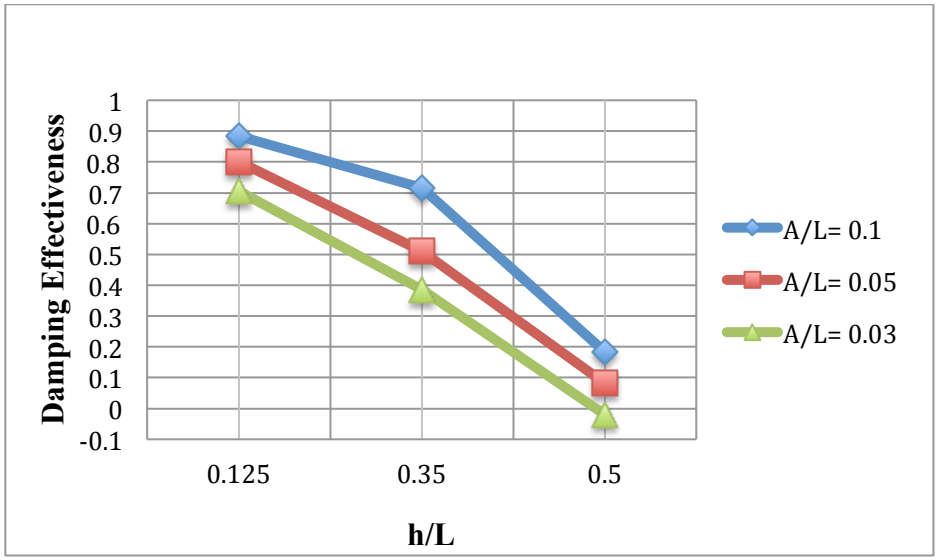

Figure 4.13 Effect of fluid height on TLD damping at f/f1=1.05 and all A/L

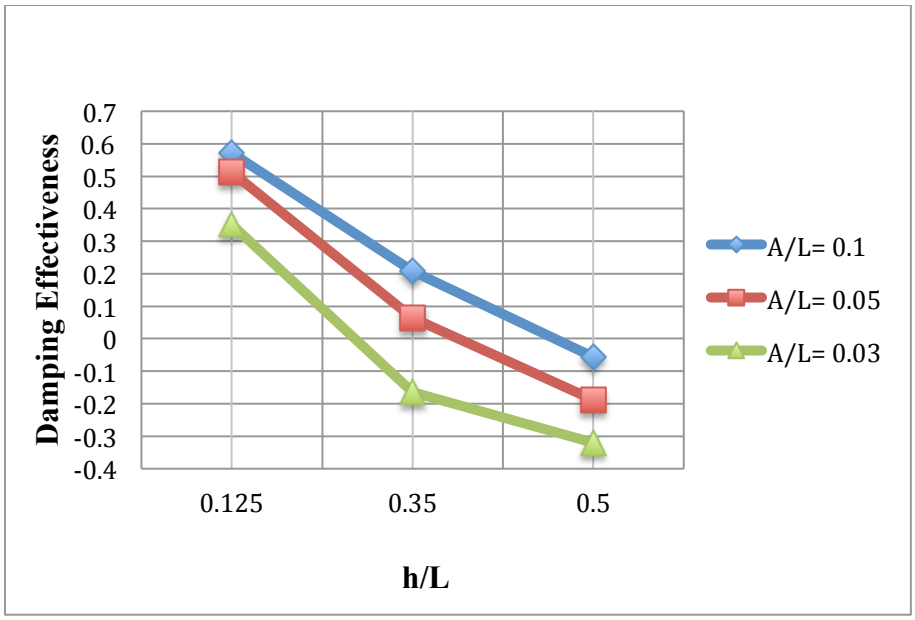

Figure 4.14 Effect of fluid height on TLD damping at f/f1=1.26 and all A/L

Figures (4.11-4.14) show that decreasing the fluid heights at any f/f1 and A/L enhances the TLD damping performance. For the highest fluid level (h/L=0.5), and at frequency ratio away from resonance, the sloshing force is in-phase with the excitation force and therefore the TLD increases the effect of the external force (negative damping; the negative numbers of damping effectiveness). The reason behind this behavior is that at highest fluid levels the major bulk of the mass does not contribute in the sloshing and as such no wave breaking happened as it was confirmed by the model at this fluid height; increasing the fluid level however, is not expected to provide any improvement in the performance of the TLD since the pressure distribution becomes almost hydrostatic. At the critical height h/L=0.35, wave starts to break at all f/f1 and A/L. The wave breaking provide more damping due to the collision between different waves along the free surface, which taking either at the mid of the tank or at walls. At h/L=0.125, more wave breaking taking place in the tank as can be seen from the wave breaking probability Figures 4.1 and 4.2. The damping increases in this shallower level that is attributed to the wave breaking.

4.5. Effect of Amplitude Ratio:

The TLD is an amplitude-dependent device i.e. increasing the amplitude increases the performance of the TLD due to increasing the sloshing force. Here in the cases examined, this trend is obvious in Figures (4.15) through (4.18).

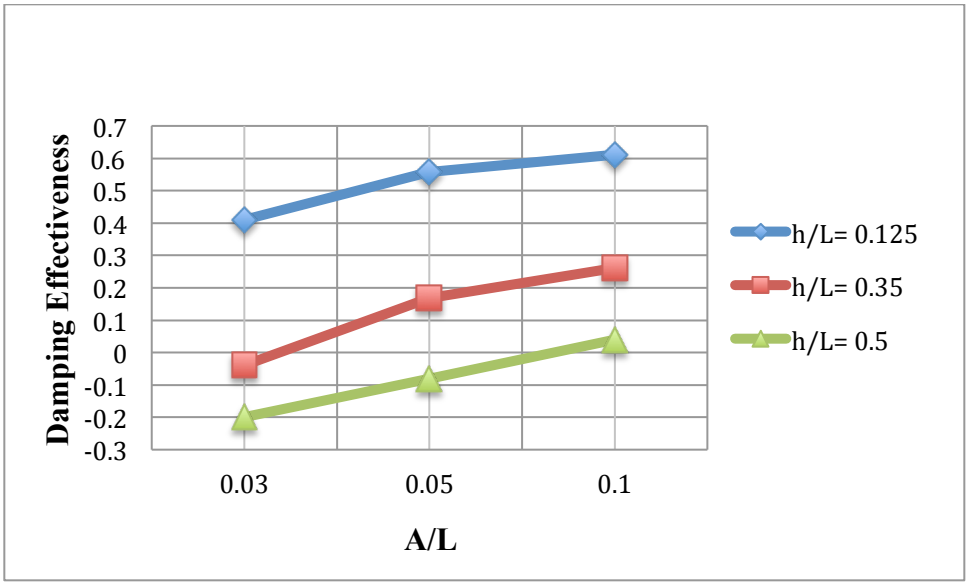

Figure 4.15 Effect of amplitude ratio on TLD damping at f/f1=0.66 and all h/L

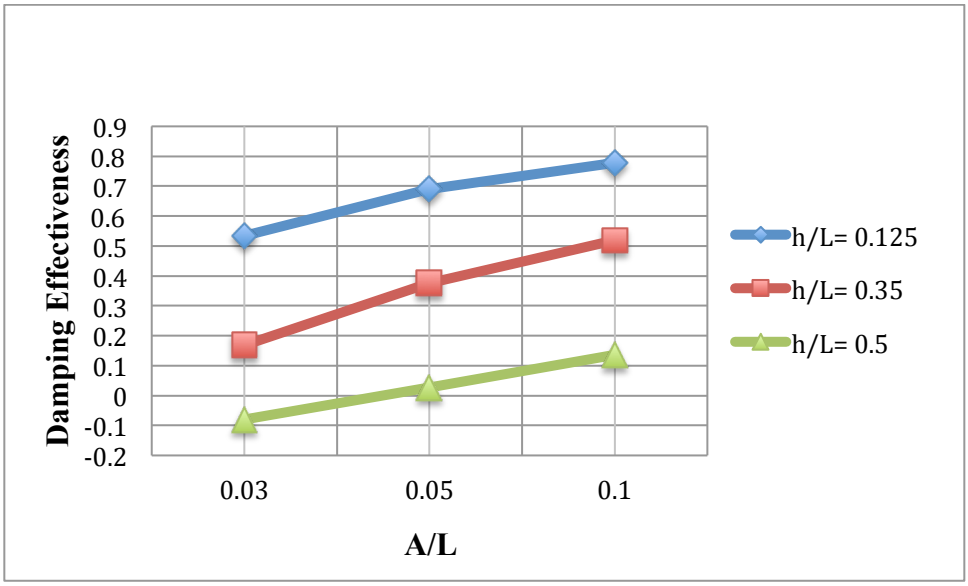

Figure 4.16 Effect of amplitude ratio on TLD Damping at f/f1=0.97 and all h/L

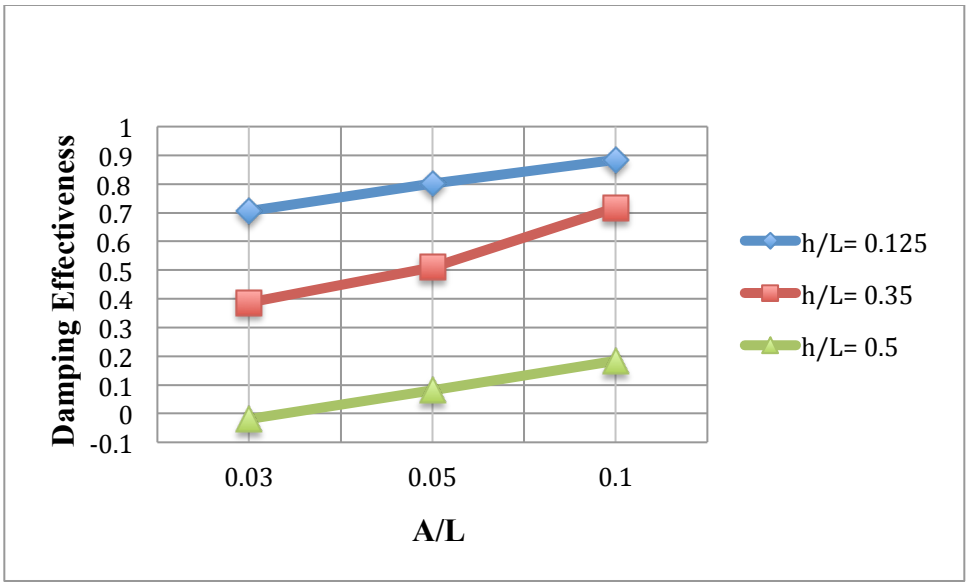

Figure 4.17 Effect of amplitude ratio on TLD Damping at f/f1=1.05 and all h/L

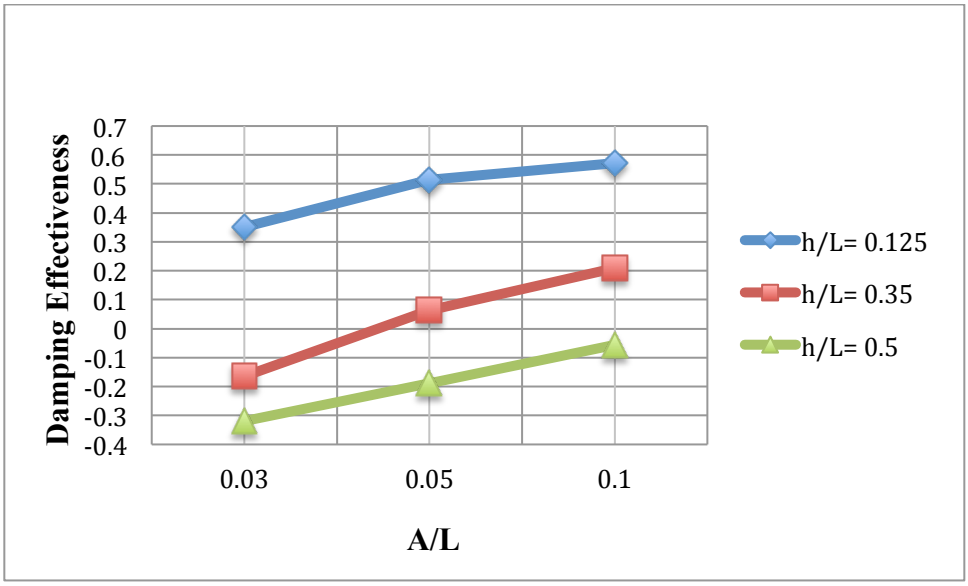

Figure 4.18 Effect of amplitude ratio on TLD Damping at f/f1=1.26 and all h/L

For the same fluid height and frequency ratio the effect of the amplitude ratio is related to the fluid height, i.e. the lesser fluid the more influential the amplitude is in terms of damping as in case of h/L=0.35 and 0.125. For these levels, increasing the amplitude ratio produces more wave breaking as seen in Figures (4.1) and (4.2). This can be attributed to the wave that propagates faster when the tank is excited with large amplitudes in the shallow levels,

and as result more fragments are formed on the surface, and consequently more damping.

4.6. Effect of Frequency Ratio:

For the three fluid heights, the TLD sloshing forces anti-phasing the excitation when in operates near the resonance as it was reported in the literature and as such the frequency ratio range was selected. The frequency ratio used in this study is the range used by Colagrossi et al (2004).

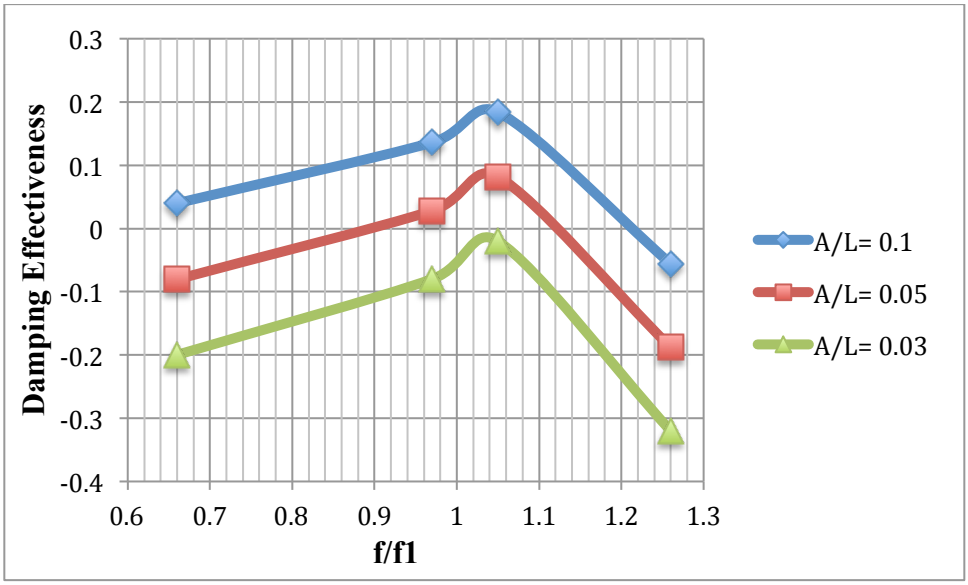

Figure 4.19 Effect of frequency ratio on TLD damping at h/L=0.5 and all A/L

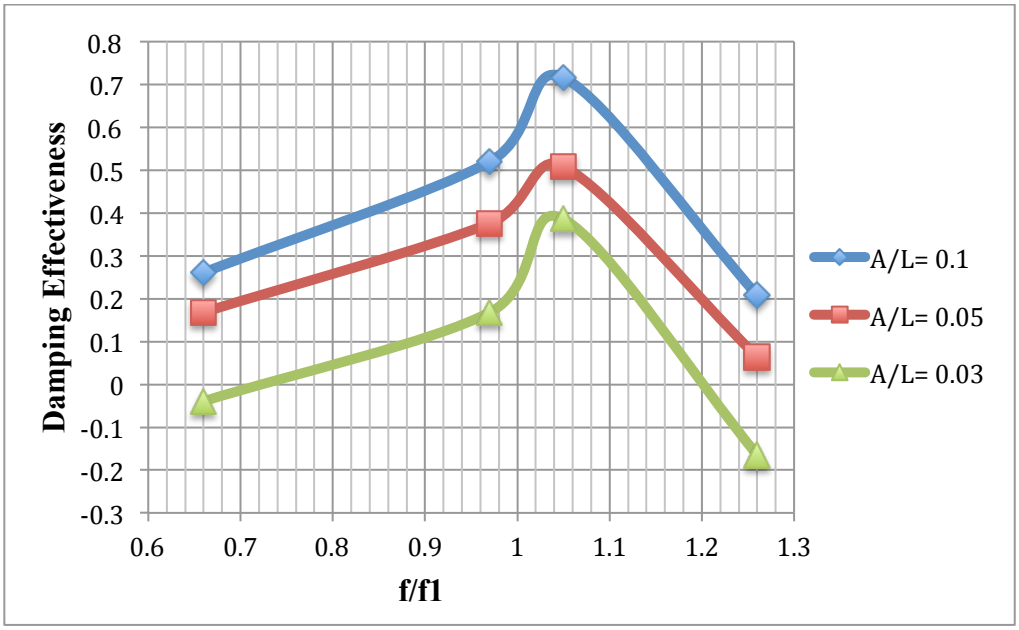

Figure 4.20 Effect of frequency ratio on TLD damping at h/L=0.35 and all A/L

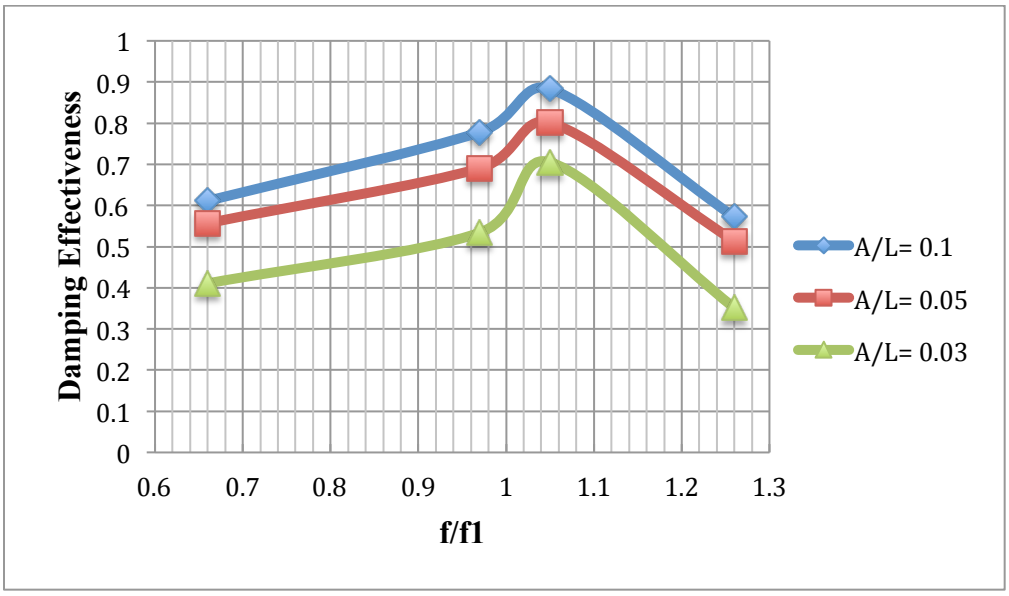

Figure 4.21 Effect of frequency ratio on TLD damping at h/L=0.125 and all A/L

As shown in Figures (4.19-4.21), the TLD performance is enhanced by increasing the frequency ratio till it reaches resonance where it starts to decay, and it would have its best damping at a frequency close to resonance; that shift is known as the jump frequency. This

trend is similar to what was reported by Reed at shallow water TLDs Reed, et al (1998). At frequency ratio of 0.66 and for all amplitude ratios considered, the TLD performs almost negatively at highest fluid level h/L=0.5 where it damps 5% of the external excitation. This percentage increases up to 25% at h/L=0.35. Lowering the fluid level even further produces more positive damping at all amplitude ratios. Similarly, the near- resonance frequencies provide more positive damping for shallow levels. The damping of the TLD starts decaying soon after frequency exceeds the jump frequency, and it is crucial at deep levels where the damping becomes negative again. The wave breaking is the main reason behind the effect of the frequency ratio on the damping trend and it can be seen clearly from the WBP in Figures (4.1-4.2). The mechanism of wave breaking in damping effectiveness driven by factors investigated (i.e. A/L, h/L, f/f1) can be explained via shear stress. The location of breaking waves is where the steep velocity gradient taking place and consequently more damping.

CHAPTER FIVE

SUMMARY AND CONCLUSIONS

Sloshing forces created due to the motion of the TLD can have positive or negative effect depending on its direction relative to the excitation forces. In this research the impact of the wave breaking due to sloshing was studied. Two main points were studied. First, the ability of the current model of representing the different wave breaking forms, that were experimentally reported, was examined. Cases for h/L= 0.35 and 0.125 for A/L=0.1 and all f/f_1were chosen. It was found that the model is capable of visualizing similar wave breaking events. Moreover, the model reported the runner-up of water along the sides of the TLD, which was not reported in Colagrossi et al (2004) as shown in the Figure (1.10). Second, the effects of different parameters on the damping effectiveness of TLD were investigated, namely fluid height (h/L), Amplitude ratio (A/L) and frequency ratio (f/f1). There fluid levels were examined (h/L=0.5, 0.35, 0.125) that represent levels above, at and less than critical fluid level ratio for the wave breaking occurrence respectively. It is concluded that the lesser the water level, the more damping the TLD provides due to the wave breaking. The attribution for this behavior is to the fact of existence a dead mass in the deep level (here h/L=0.5) which does not benefit the damping of the TLD, on the other hand, levels close to critical fluid height ratio enhance the damping because of the wave breaking that is recorded to take place at all amplitude and frequency ratios (Figures (4.1) and (4.2)). The amplitude ratio is an important factor in the performance of the TLD. Three amplitude ratios were used (A/L= 0.1, 0.05, 0.03). It is concluded from the cases run in this research that increasing the amplitude ratio leads to higher damping regardless of the fluid height and frequency ratio. The influence of the amplitude ratio becomes more dominant at the shallower levels i.e. h/L=0.125. The frequency ratio is of great importance of this study. Since

TLDs are devices preferably working near resonance, as such the frequency ratio range (f/f_1= 0.66, 0.97, 1.05, 1.26) was selected. Increasing the frequency ratio increases the amount of the wave breaking as it is noted in Figures (4.1) and (4.2). Near resonance is where the TLD would have its upmost damping effectiveness; afterwards, the damping effectiveness of the TLD starts to deteriorate. In the range of the frequency ratio selected the f/f_1= 1.05 is concluded as the best frequency ratio in terms of damping effectiveness. Additionally, the higher amplitude ratio i.e. A/L=0.1 is the best amplitude ratio value in providing the best damping effectiveness. It turns out that the fluid height h/L=0.125, which was reported as the best fluid level that reduces the motion of the structure Venkateswara Rao K (2013), is the best fluid level used in this study to provide damping by the TLD.

CHAPTER SIX

RECOMMENDATION FOR FUTURE WORK

The effect of the wave breaking on the performance of the TLD was studied under several factors and assumptions; the wave breaking was found to have a significant impact on the performance of the TLD. The following are some suggestions for future work for those who are interested in the same topic:

1. The TLD used was a simple rectangular tank, other tank configurations are recommended to examine such as in case of space limitation (irregular shapes).
2. The model was developed for 2D flow; the pursers might want to consider the 3D cases.
3. The effect of the wave breaking on the structure should be investigated by coupling the TLD with a structure.

Reference

Alfriend, K. T. (1974). "Partially filled viscous ring nutation damper", *J. Spacecraft Rockets*, 11, 456-462

Bauer, H.F. (1984)." New Proposed Dynamic Vibration Absorbers for Excited Structures," *Vibration Damping Workshop Proceedings*, 1-27.

Banerji, A. S. (2011). "Earthquake vibration control of structures using hybird mass liquid damper," *Engineering Structures*, 1291-1301.

Banerji, M. M. (1999). "Tuned liquid dampers for controlling earthquake response of structures," *Earthquake Engineering And Structural Dynamics*, 587-602.

Bouscasse, M. A. (2013). "Numerical and Experimental Investigation of Nonlinear Shallow Water Sloshing," *Int. J. Nonlinear Science Numerical Simulation,* 14, 123–138.

Bhattacharyya, P. P. (2010). "Sloshing in partially filled liquid containers-numerical and experimental study for 2D problems," *Journal of sound and vibration*, 4466-4485.

Bhattacharjee, E., Halder, L., and Sharma, R. P. (2013). "An experimental study on tuned liquid damper for mitigation of structural response," *International Journal of Advanced Structural Engineering*.

Bhuta, P.G. and Koval, L.R. (1966)." A Viscous Ring Damper for a Freely Processing Satellite," *International Journal of Mechanical Science,* 8, 383-395.

Bones, A. and Chester, W. (1968). "Resonant oscillation of water waves," *Mathematical and physical sciences,* 306, 23-39.

Brackbill, D. B. (1992). "A Continuum Method for Modeling Surface Tension," *Journal of Computational Physics,* 100, 335-354.

Casciati, A. D. (2003). "Simulating a conical tuned liquid damper," *Simulation Modeling Practice and Theory*, 11, 353-370.

Chang, C.C and Gu, M. (1999). "Suppression of vortex-excited vibration of tall building using tuned liquid dampers," *Wind Engineering and Industrial Aerodynamics,* 83, 225-237.

Chorin, A. J. (1968). "Numerical Solution of The Navier Stockes Equations," *Mathematics of Computation,* 22 (104), 745-762.

Colagrossi, A. (2004). "A Meshless Lagrangian Method for Free–Surface and Interface Flows with Fragmentation," PhD Thesis, Universita di Roma La Sapienza.

Colagrossi, A., Palladino, F and C. Greco. (2004). "Experimental and Numerical investigation of 2D sloshing: scenarios near the critical filling depth," International Workshop on water waves and floating body.

Colagrossi, A., Brocchini, M. and Lugni, C. (2010). "A study of violent sloshing wave impacts using an improved SPH method," Journal of Hydraulic Research, 48, 94–104.

Delorme, L., Colagrossi, A., Souto-Iglesias, Zamora-Rodríguez, R. and Botía-Vera, E. (2009). "A set of canonical problems in sloshing, Part I: Pressure field in forced roll—comparison between experimental results and SPH," *Ocean Engineering,* 36, 168-178.

Fang, J., Parriaux, A., Rentschler. M. and Ancey, M. (2009). "Improved SPH methods for simulating free surface flows of viscous fluids," Applied Numerical Mathematics, 59, 251-271.

Frahm, H. (1911). "Device for Damping Vibrations of Bodies" United States Patent Office Patent No. 989958.

Fujii, K., Tamura, Y., Sato, T. and Wakahara, T. (1990). "Wind-induced vibration of tower and practical applications of tuned liquid damper," *Journal of Wind Enginering and Aerodynamics,* 33, 263–72.

Graham, E. W. (1951). "The forces produced by fuel oscillation in a rectangular tank*,"* Santa Monica, Calif, USA: Douglas Aircraft Company.

Graham, E. W., Rodriquez, A. M. (1952). "The Characteristics of Fuel Motion which Affect Airplane Dynamics," *Journal of Applied Mechanics*, 381-388.

Gao, H., Kwok, K.C.S. and Samali, B. (1997). "Optimization Of Tuned Liquid Column Dampers," Engineering Structures, 19 (6), 476-486.

Honkanen, M.G. (1990). " Heel and Roll Control by Water Tank", Naval Architect, 215-216.

Hirt, B. D. (1981). "Volume of Fluid (VOF) Method for the Dynamics of Free Boundaries," *Journal of Computational Physics, 39*, 201-225.

Hitchcock, P., Kwok, K.C.S., Watkins, R.D. and Samali, B. (1997). "Characteristics Of Liquid Column Vibration Absorbers (LCVA)-I," *Engineering Structures,* 19 (2), 126-134.

Ju, Y. K. Yoon. S. W. and Kim, S. D. (2004). "Experimental Evaluation of Tuned Liquid Damper system," *Structures and Buildings,* 157, 251-262.

Jin, Q., Li, X., Sun, N., Zhou, J. and Guan, J. (2007). "Experimental And Numerical Study On Tuned Liquid Dampers For Controlling Earthquake Response Of Jacket Offshore Platform," *Marine Structures*, 238-254.

Kareem, A. (1990). "Reduction of Wind Induced Motion Utilizing a Tuned Sloshing Damper," *Journal of Wind Engineering and Industrial Aerodynamics*, 36, 725-37.

Kareem, A. and Sun, W.J (1987). "Stochastic Response Of Structures With Fluid-Containing Appendages," *Journal of Sound and Vibration*, 119 (3), 389-408.

Kaneko. S. and Ishikawa, M. (1999). "Modeling of Tuned Liquid Damper With Submerged Nets," *Journal of Pressure Vessel Technology,* 121, 334-343.

Kim, Y., You, K., Cho, J. and Hong, D (2006). "The Vibration Performance Experiment of Tuned Liquid Damper and Tuned Liquid Column Damper," *Journal of Mechanical Science and Technology,* 20, 795-805.

Kwok, K.C.S and Samali, B. (1995). "Performance Of Tuned Mass Dampers Under Wind Loads," *Engineering Structures,* 17, 655-667.

Kareem, A. (1993). "Liquid Tuned Mass Damper: Past, Present, Future," *Proceeding of the 7th U.S. National Conference on Wind Engineering*.

Khezzar, L., Seibi, A.C. and Afshin, G. "Water Sloshing in Rectangular Tanks An Experimental Investigation & Numerical Simulation," *International Journal of Engineering,* 3 (2), 174-184.

Lamb. (1945). "Hydrodynamics," (Sixth edition), New York, USA: Dover.

Lamb. (1932). "Hydrodynamics," Cambridge University Press. London. England.

Lepelletier, T. and Raichlen, F. (1988). "Nonlinear Oscillations In Rectangular Tanks," Journal of Engineering Mechanics, 114, 1-23.

Lin, P. Liu, P. (1997). "A Numerical Model For Breaking Waves: The Volume Of Fluid Method*,"* University of Delware, Ocean Engineering Laboratory.

Lin, P. (2008). "Numerical Modeling Of Water Waves," Taylor and Francis. NewYork, USA.

Lugni, C., Colagrossi, A., Greco, M. and Faltinsen, O. M. (2004). "Experimental and numerical investigation of 2D sloshing with slamming," *19th International Workshop on Water Waves and Floating Body*. Cortona, Italy: INSEAN, Italian Ship Model Basin.

Liu, D. and Lin, P. (2008). "A Numerical Study Of Three Dimensional Liquid Sloshing In Tanks," *Journal of computational Physics,* 227, 3921-3939.

McKee, S., Tome, M.F., Ferreira, V.G., Cuminato, J.A., Castelo, A., Sousa, F.S. and Mangiavacchi, N. (2007). "Review The MAC Method," *Computers and Fluids,* 37, 907-930.

Marivani, M. and Hamed, M. S. (2009). "Numerical Investigation Of Sloshing Motion Inside Tuned Liquid Dampers With And Without Submerged Screens," PhD Thesis, McMaster University, Canada.

Mimi, G. (2011). "Numerical Simulation Of Liquid Sloshing In Rectangular Tanks Using Consistent Particle Method And Experimental Verification." PhD Thesis. National University Of Singapore.

Mitome, S and Vandiver, J. K. (1979). " Effect Of Liquid Storage Tanks On The Dynamic Response Of Off Shore Platforms," *Applied Ocean Research*, 1, 67–74.

Modi V. J, Welt, F. (1988). "Damping Of Wind Induced Oscillations Through Liquid Sloshing," *Journal of Wind Engineering and Industrial Aerodynamics*, 30, 85–94

Monaghan, J. (1988). "An Introduction to SPH," *Computer Physics Communications*, 48, 89-96.

Morsy, H. (2010). "A Numerical Study of the Performance of the Tuned Liquid Dampers," M.A.Sc Thesis, McMaster University, Canada.

Mohamed S. Hamed., Saud Ghani. 2014. *Numerical and Experimental Investigation of Performance of Tuned Liquid Dampers*. Qatar University, Report No. NPRP 09-769-2-292. Doha, Qater.

Ibrahim. (2005). "Liquid Sloshing Dynamics: Theory and Applications," . New York , New York , USA: Cambridge University Press .

Panigrahy, P.K., Saha, U.K. and Maity, D. (2009). "Experimental Studies On Sloshing Behavior Due To Horizontal Movement Of Liquids In Baffled Tanks," *Ocean Engineering*, 36, 213–222.

Price WG and Chen, Y. G. (2006). "A Simulation Of Free Surface Waves For Incompressible Two- Phase Flows Using A Curvilinear Level Set Formulation," Int Journal of Numerical Methods Fluids, 51 (3), 305–30.

Rao, S. S. (2011). "Mechanical Vibration," (5th edition). per Saddle River, NJ, USA: Pearson.

Reed, D. Y., Yu, J., Yeh, H. and Gardarsson, S. (1998). "Investigation Of Tuned Liquid Dampers Under Large Amplitude Excitation," *Journal of Engineering Mechanics,* 124, 405-413.

Schneider, C. C. and Likins, P. W. (1973). "Nutation dampers versus pre- cession dampers for axisymmetric spinning spacecraft", *J. Spacecraft Rockets*, 10, 218-222

SeiIchi, K., Atsushi, N and Yoshiaki, O. (1997). "Numerical Analysis Of Breaking Waves Using The Moving Particle Semi-Implicit Method," *International Journal For Numerical Methods In Fluids,* 26, 751–769.

Siddique, M. R., Hamed, M. S. and El Damatty, A. A. (2004). "A nonlinear numerical model for sloshing motion in tuned liquid dampers," International Journal for Numerical Methods in Heat & Fluid Flow, 15 (3), 306-324.

Souto-Iglesiasa, A., Delormea, L., Pérez-Rojasa, L and Abril-Pérezb, S. (2006). "Liquid moment amplitude assessment in sloshing type problems with smooth particle hydrodynamics," *Ocean Engineering,* 33, 1462-1484.

Souto Iglesias, A., Pérez Rojas, L. and Zamora Rodríguez, R. (2004). "Simulation of anti-roll tanks and sloshing type problems with smoothed particle hydrodynamics," *Ocean Engineering,* 31, 1169-1192.

Soong, T. T. and Dargush, G. F. (1997). "Passive Energy Dissipation Systems in Structural Engineering", John Wiley & Sons: West Sussex, England.

Sun, L., Fujino, Y., Pacheco, B. and Isobe M. (1989). "Nonlinear Waves And Dynamic Pressure In Rectangular TLD- Simulation And Experimental Verification," *JSCE Structural engineering, earthquake engineering*, 6, 251-262.

Sun, L. (1991). "Semi-Analytical Modelling of TLD With Emphasis on Damping of Liquid Sloshing", Ph.D., University of Tokyo, Japan,

Sun, L., Fujino, Y., Pacheco, B. and Chaiseri, P. (1992). "Modeling of Tuned Liquid Damper (TLD)," *Journal of Wind Engineering and Industrial Aerodynamics,* 41, 1883-1894.

Sun, L. and Fujino, Y. (1994). "A Semi-Analytical Model For Tuned Liquid Damper (TLD) With Wave Breaking," *Journal of fluids and structures*, 8, 471-488.

Sun, L., Fujino, Y., Chaiseri, P. and Pacheco, B (1995). "The Properties Of Tuned Liquid Dampers Using A TMD Analogy," *Earthquake engineering and structure dynamics*, 24, 967-976.

Tait, M.J. and Love J.S. (2012). "A Preliminary Design Method For Tuned Liquid Dampers Conforming To Space Restrictions," *Engineering Structures,* 40, 187-197.

Tait, M. J. Love, J. S. and Nezhad, H. (2010). "A Hybrid Structural Control System Using A Tuned Liquid Damper To Reduce The Wind Induced Motion Of A Base Isolated Structure," *Engineering structures*, 33, 738-746.

Tamura, Y., Fujii, K., Ohtsuki, T., Wakahara, T. and Kohsaka, R., (1995). "Effectiveness of Tuned Liquid Dampers Under Wind Excitation", *Journal of Engineering Structures*, 17, 609-621.

Taipei-101. (2009). "Taipei-101 Observatory," Retrieved April 20, 2013, from http://www.taipei-101.com.tw.

Venkateswara Rao K (2013). "Experimental And Numerical Studies On Tuned Liquid Damper," M. A. Sc. Thesis. National Institute Of Technology Rourkela, Orissa, Department Of Civil Engineering.

Warburton, G. (1982). "Optimum Absorber Parameters For Various Combinations of Response& Excitation Parameters," Earthquake Engineering and Structure Dynamics,10, 381-401.

Wakahara, T., Ohyama, T. and Fujii, K. (1992). "Suppression of Wind- Induced Vibration of a Tall Building using Tuned Liquid Damper." *Journal of Wind Engineering and Industrial Aerodynamics*, 41, 1895-1906.

Welch, J. and Harlow, F. (1965). "Numerical Calculation of Time-Dependent Viscous Incompressible Flow of Fluid with Free Surface," *The Physics of Fluids, 8*, 2182-2189.

Wang, G., Yi, T., Jing, Q., Huo, L and Li, H. (2011). "Wind-Induced Vibration Control of Dalian International Trade Mansion by Tuned Liquid Damper," *Mathematical Problems in Engineering*, 2012, 1-21.

Yu, J. K. (1997). "Non-Linear Characteristics of Tuned Liquid Dampers," PhD Thesis. University of Washington.

Zhang, Z., Li, A., He, J. and Wang, J. (2009). "Wind-Induced Vibration Control Of Hefei TV Tower With Fluid Viscous Damper," Translated from Journal of southeast University, 249-254.